

# Synthesis of Diarylpentadienones and Pyrazoline Derivatives as Potential $\alpha$ -Glucosidase Inhibitor and Their Antioxidant Activities

Faruk Auwal Adam<sup>1</sup>, Mohammad Aidiel Md Razali<sup>1</sup>, Yaya Rukayardi<sup>2,3</sup>, Siti Nurulhuda Mastuki<sup>2</sup>, Leong Sze Wei<sup>2</sup>, Nadiyah Mad Nasir<sup>1</sup> and Siti Munirah Mohd Faudzi<sup>1,2,\*</sup>

<sup>1</sup>Department of Chemistry, Faculty of Science, Universiti Putra Malaysia, 43400 Serdang, Selangor, Malaysia

<sup>2</sup>Natural Medicines and Products Research Laboratory, Institute of Bioscience, Universiti Putra Malaysia, 43400 Serdang, Selangor, Malaysia

<sup>3</sup>Department of Food Science, Faculty of Food Science and Technology, Universiti Putra Malaysia, 43400 Serdang, Selangor, Malaysia

\*Corresponding author (e-mail: sitimunirah@upm.edu.my)

Diabetes mellitus type II (T2DM) is a global public health crisis that can lead to death and disability if poorly treated. T2DM patients are usually prescribed antidiabetic drugs, including  $\alpha$ -glucosidase inhibitors (AGIs), but their use can lead to complications. Epidemiological studies have already shown that antioxidant compounds are able to scavenge reactive species and alleviate oxidative stress in T2DM patients. With the main objective of improving the quality of life of T2DM patients, a series of diarylpentadienones (**3a-j**) and their new pyrazoline derivatives (**4a-i**) were synthesized and evaluated for their  $\alpha$ -glucosidase inhibition and antioxidant abilities. The results showed that 5-(4-methoxyphenyl)-1-(5-methylthiophen-2-yl)penta-2,4-dien-1-one (**3h**) exhibited significant  $\alpha$ -glucosidase inhibition ( $IC_{50}$   $40.52 \pm 2.0 \mu\text{M}$ ) compared to the standard drug acarbose ( $IC_{50}$   $543.80 \pm 3.0 \mu\text{M}$ ). While 1-(2,4-dimethoxyphenyl)-5-(4-methoxyphenyl)penta-2,4-dien-1-one (**3d**) and 1-(3-(3-fluorophenyl)-5-(4-methoxystyryl)-4,5-dihydro-1H-pyrazol-1-yl)ethenone (**4f**) showed promising radical scavenging potentials of DPPH (96-97%) and NO (8-74%), which were comparable to the control compounds, quercetin and gallic acid. Molecular docking simulations were then performed to reveal several significant binding interactions of the active molecules with the corresponding protein crystals. It can be concluded that diarylpentadienone and its pyrazoline derivatives are molecules with potential anti- $\alpha$ -glucosidase and antioxidant properties, but not as dual active compounds, suitable for possible chemical modification according to pharmaceutical requirements in the future.

**Keywords:** Diarylpentadienone; pyrazoline;  $\alpha$ -Glucosidase inhibitor; antioxidant; molecular docking

Received: November 2022; Accepted: December 2022

Diabetes mellitus (DM) is a global health problem with a prevalence of 9.3% (463 million people) in 2019 and is expected to increase to 10.2% (578 million) by 2030 and 10.9% (700 million) by 2045 [1]. It is a chronic and progressive disease characterized by high blood glucose levels. When the condition persists for a long time and inadequately treated, diabetes can lead to various complications such as myocardial infarction, renal failure, amputation, and vision loss [2]. DM is profound towards type 2 diabetes mellitus (T2DM), which occurs in 90% of diabetics and is currently a leading cause of morbidity and mortality worldwide. T2DM is often the result of insulin resistance, which in turn impairs the body's glucose metabolism [3]. Scientists have demonstrated that  $\alpha$ -glucosidase, a catalytic enzyme involved in the cleavage of 1,4- $\alpha$ -glycosidic bonds in starch and disaccharides and subsequently converting them to glucose, is one of the culprits of diabetes [4].

People suffering from T2DM are usually

prescribed different classes of drugs to regulate their blood glucose levels, including biguanides, sulfonamide, thiazolidinediones, meglitinides,  $\alpha$ -glucosidase inhibitors (AGIs), and DPP-4 inhibitors. However, most of these pharmacotherapies are unsatisfactory and often associated with adverse side effects [5]. Therefore, the development of new AGI candidates is necessary to avoid complications in the current and future treatment of T2DM and has been an attractive topic for pharmaceutical research for the last two decades [6].

AGIs are antihyperglycemic agents that block the action of enzymes that normally break down carbohydrates [7]. AGIs have already been shown to be useful in the treatment of diabetic patients with postprandial hyperglycemia (PPHG). Inhibition of the activity of the enzyme  $\alpha$ -glucosidase leads to a reduction in starch hydrolysis, which has a positive effect on the regulation of the glycemic index in diabetic patients [8]. Interestingly, antioxidants, i.e., *N*-

acetylcysteine and vitamin C, have proven to contribute to the reduction of diabetic complications, suggesting that they may be helpful as dietary supplements [9].

Antioxidants are molecules that prevent or significantly slow down the oxidation of substances in small amounts in the body [10] and are responsible for an organism's defense mechanism against pathogens associated with free radical attacks. The major oxygenated free radicals or reactive oxygen species (ROS) involved in many diseases include hydroxyl, superoxide anion, nitric oxide, and peroxyxynitrite radicals [11]. On the other hand, nitric oxide, peroxyxynitrous acid, peroxyxynitrite, and nitrogen dioxide are examples of nitrogen-containing free radicals called reductive nitrogen species or RNS [12]. These free radicals are produced internally as by-products of regular important metabolic processes such as the electron transport reaction catalyzed by mitochondria and the inflammatory reactions of neutrophils and macrophages. It is worth mentioning that the intake of antioxidants is involved in the prevention of degenerative diseases caused by oxidative stress, such as atherosclerosis [12], cancer [13], Parkinson's disease [14] or Alzheimer's disease [15].

Diarylpentadienones, a new class of compounds derived from curcuminoids, are potential pan-assay interference compounds (PAINS) because they consist of a reactive  $\alpha,\beta$ -unsaturated C5 linker. Previous studies have shown that this class of compounds have excellent bioavailability and pharmacological activities such as anti-inflammatory, antioxidant and  $\alpha$ -glucosidase inhibitory properties [16, 17, 18, 19]. All these remarkable properties allow them to be used to treat a variety of chronic diseases such as cancer, diabetes, and neurodegenerative diseases. Therefore, diarylpentadienones can be considered as potential candidates for new drug development. However, identification of possible PAINS substructures in the designed compounds before experimental synthetic work was essential to validate the predicted role of the molecules of interest and avoid any ambiguous details. On the other hand, pyrazolines are two adjacent nitrogen atoms within the ring of a five-membered heterocyclic molecule. Pyrazolines are basic in nature and have only one endocyclic double bond [20]. Pyrazoline derivatives exhibit beneficial biological

effects such as antimicrobial [21], anti-tumour [22], anti-tuberculous [23], anti-inflammatory [24], antioxidant [25], and antidepressant [26] activities.

In search of new drug candidates with significant dual action in reducing diabetic complications and as antioxidants, a series of diarylpentadienones (**3**) and their new pyrazoline derivatives (**4**) (Figure 1) were PAINS-filtered, synthesized, and biologically screened for their  $\alpha$ -glucosidase suppression and antioxidant activity. The most active molecules were then subjected to molecular docking experiments to gain insight into the binding interaction between the ligand and the specific active sites to better understand their  $\alpha$ -glucosidase inhibition and antioxidant properties. It is worth mentioning that several diarylpentadienones and their pyrazoline derivatives have already been synthesized and described [27, 28, 29]. However, their antidiabetic and nonenzymatic antioxidant properties, especially inhibition of  $\alpha$ -glucosidase, DPPH, and NO radical scavenging, have never been reported. It should be noted once again that the NO radical scavenging results explained in this work are used to evaluate the antioxidant potential of the synthesized compounds and not their anti-inflammatory potential, as previously reported in [27, 29].

## EXPERIMENTAL

### Chemistry

All commercially available chemicals, reagents, and organic solvents were purchased from Sigma Aldrich, R&M Chemicals, and Avocado and used without additional purification. Thin layer chromatography (0.20mm Merck silica gel 60 F254 TLC plate) was regularly performed to monitor the reaction processes at each reaction stage, while column chromatography on silica gel was used for purification purposes with a polarity gradient manner. Various spectroscopic instruments were adopted for structural characterization, including high-resolution MS (HRMS) was recorded using an Acquity Ultra-Performance Liquid Chromatography (UPLC) PDA system coupled to a Synapt High-Definition Mass Spectrometry (HDMS) quadrupole-orthogonal) acceleration time-of-flight (oa-TOF)

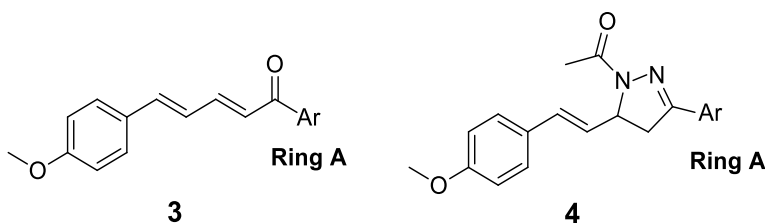


**Figure 1.** General structure of diarylpentadienone (series **3**) and its pyrazoline derivatives (series **4**)

detector (Waters Corporation, USA) and equipped with an ESI source. Nuclear magnetic resonance spectra were recorded using a Varian 500 MHz NMR spectrometer (Palo Alto, USA) and FTIR spectra were recorded using a Perkin Elmer RX1 FTIR spectrometer (Massachusetts, USA) in the mid-range IR (400-4000  $\text{cm}^{-1}$ ). The melting points of all synthesized molecules were measured using the conventional Fisher-Johns melting point instrument.

### General Procedure for the Synthesis of Series 3

Equimolar amounts of 4-methoxycinnamaldehyde (2 mmol) and substituted acetophenone (2 mmol) were dissolved in 5 mL of ethanol. The mixed solution was then homogeneously mixed for five minutes before 6M NaOH (1 mL) was slowly added and stirred at room temperature for the next 24 hours. The solution was poured into crushed ice and neutralised with dilute HCl to stop the reaction. The resulting mixture was extracted three times with ethyl acetate (10 mL), dried over anhydrous  $\text{MgSO}_4$ , and evaporated by rotary evaporation to afford the crude products, which were then purified by column chromatography with hexane and ethyl acetate in a polarity gradient to afford the pure **3a-j** products [27]. All compounds were then sent for spectroscopic analysis for structure confirmation. The 1-dimensional  $^1\text{H}$ - and  $^{13}\text{C}$ -NMR spectra were measured in deuterated chloroform ( $\text{CDCl}_3$ ), with chemical shifts reported in  $\delta$  (ppm) values relative to the standard tetramethylsilane (TMS). The visualisation of NMR spectra and data analysis were performed using the software package MestReNova version 6.0.2-5475, and the numbering of the carbons/hydrogens in the series **3** structure used in the NMR analysis is shown in Figure 2.

#### 5-(4-Methoxyphenyl)-1-phenylpenta-2,4-dien-1-one (3a)

Yellow solid 61% yield; m.p. 110-111 $^\circ\text{C}$ .  $^1\text{H}$ -NMR (500 MHz,  $\text{CDCl}_3$ ):  $\delta$  7.97 (d, 2H,  $J = 7.4$  Hz, H-2', H-6'), 7.65 – 7.53 (m, 2H, H-2'', H-6''), 7.47 (dd, 4H,  $J = 15.4, 8.2$  Hz, H-3', H-4', H-5', H-4), 7.05 (d, 1H,  $J_{trans} = 14.9$  Hz,

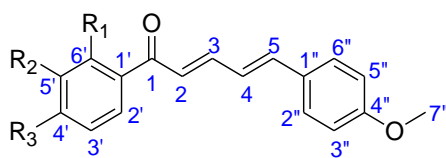
H-2), 6.98 (d, 1H,  $J_{trans} = 15.5$  Hz, H-5), 6.95 – 6.87 (m, 3H, H-3'', H-5'', H-3), 3.84 (s, 3H, H-7'').  $^{13}\text{C}$ -NMR (126 MHz,  $\text{CDCl}_3$ ):  $\delta$  190.4 (C-1), 160.6 (C-4''), 145.4 (C-2), 141.9 (C-5), 138.4 (C-4), 132.6 (C-3), 128.9 (C-1'), 128.8 (C-2', C-6'), 128.5 (C-3', C-5'), 128.3 (C-2'', C-6''), 124.8 (C-1''), 124.2 (C-4'), 114.3 (C-3'', C-5''), 55.3 (C-7''). HRMS (ESI):  $m/z$  calcd for  $\text{C}_{18}\text{H}_{16}\text{O}_2\text{-H}$ : 263.1421 [M-H] $^-$ ; found: 263.1524.

#### 1-(3-Methoxyphenyl)-5-(4-methoxyphenyl)penta-2,4-dien-1-one (3b)

Yellow solid 74% yield; m.p. 85-86 $^\circ\text{C}$ .  $^1\text{H}$ -NMR (500 MHz,  $\text{CDCl}_3$ ):  $\delta$  7.60 (dd, 1H,  $J_{trans} = 14.9, 10.7$  Hz, H-3), 7.55 (d, 1H,  $J = 7.6$  Hz, H-2'), 7.51 (d, 1H,  $J = 2.1$  Hz, H-6'), 7.45 (d, 2H,  $J = 8.7$  Hz, H-2'', H-6''), 7.39 (t, 1H,  $J = 7.9$  Hz, H-2'), 7.11 (dd, 1H,  $J = 8.2, 2.6$  Hz, H-4'), 7.03 (d, 1H,  $J_{trans} = 14.9$  Hz, H-2), 6.98 (d, 1H,  $J_{trans} = 15.5$  Hz, H-5), 6.94 – 6.89 (m, 3H, H-3'', H-5'', H-4), 3.88 (s, 3H, H-7'), 3.84 (s, 3H, H-7'').  $^{13}\text{C}$ -NMR (126 MHz,  $\text{CDCl}_3$ ):  $\delta$  190.2 (C-1), 160.5 (C-5'), 159.8 (C-4''), 145.4 (C-2), 141.8 (C-5), 139.7 (C-1'), 129.4 (C-4), 128.9 (C-3), 128.8 (C-2'', C-6''), 124.8 (C-3'), 124.2 (C-1''), 120.8 (C-4'), 119.1 (C-6'), 114.3 (C-3'', C-5''), 112.5 (C-2'), 55.4 (C-7'), 55.3 (C-7''). HRMS (ESI):  $m/z$  calcd for  $\text{C}_{19}\text{H}_{18}\text{O}_3\text{-H}$ : 293.2012 [M-H] $^-$ ; found: 293.2017.

#### 1,5-Bis(4-methoxyphenyl)penta-2,4-dien-1-one (3c)

Yellow solid 90% ; m.p. 107-108 $^\circ\text{C}$ .  $^1\text{H}$ -NMR (500 MHz,  $\text{CDCl}_3$ ):  $\delta$  8.00 (d, 2H,  $J = 8.8$  Hz, H-2', H-6'), 7.60 (dd, 1H,  $J_{trans} = 14.8$  Hz, H-3), 7.46 (d, 2H,  $J = 8.7$  Hz, H-3', H-5'), 7.07 (d, 1H,  $J_{trans} = 14.8$  Hz, H-2), 7.01 – 6.95 (m, 3H, H-2'', H-6'', H-H-4), 6.95 – 6.88 (m, 3H, H-3'', H-5''), 3.89 (s, 3H, 7'), 3.85 (s, 3H, H-7'').  $^{13}\text{C}$ -NMR (126 MHz,  $\text{CDCl}_3$ ):  $\delta$  188.7 (C-1), 163.2 (C-4'), 160.4 (C-4''), 144.5 (C-1'), 141.2 (C-2), 131.2 (C-3), 130.6 (C-2', C-6'), 129.0 (C-5), 128.7 (C-3', C-5') 124.9 (C-1''), 124.1 (C-4), 114.2 (C-2'', C-6''), 113.75 (C-3'', C-5''), 55.4 (C-7'), 55.3 (C-7''). HRMS (ESI):  $m/z$  calcd for  $\text{C}_{19}\text{H}_{18}\text{O}_3\text{-H}$ : 293.2013 [M-H] $^-$ ; found: 293.2015.



- 3a:**  $\text{R}_1 = \text{R}_2 = \text{R}_3 = \text{H}$   
**\* 3b:**  $\text{R}_2 = \text{OCH}_3$ ;  $\text{R}_1 = \text{R}_3 = \text{H}$   
**3c:**  $\text{R}_3 = \text{OCH}_3$ ;  $\text{R}_1 = \text{R}_2 = \text{H}$   
**3d:**  $\text{R}_1 = \text{R}_3 = \text{OCH}_3$ ;  $\text{R}_2 = \text{H}$   
**\* 3e:**  $\text{R}_1 = \text{F}$ ;  $\text{R}_2 = \text{R}_3 = \text{H}$   
**\* 3f:**  $\text{R}_2 = \text{F}$ ;  $\text{R}_1 = \text{R}_3 = \text{H}$   
**3g:**  $\text{R}_3 = \text{F}$ ;  $\text{R}_1 = \text{R}_2 = \text{H}$   
**\* 3j:**  $\text{R}_1 = \text{F}$ ;  $\text{R}_2 = \text{H}$ ;  $\text{R}_3 = \text{OCH}_3$

\* New compounds

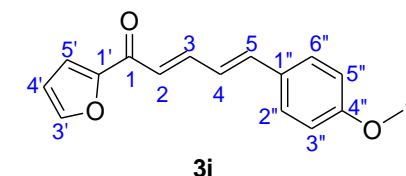
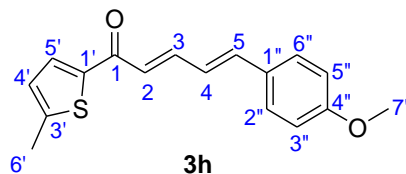


Figure 2. Chemical structures of series 3

**1-(2,4-Dimethoxyphenyl)-5-(4-methoxyphenyl)penta-2,4-dien-1-one (3d)**

Yellowish orange solid 91%; m.p. 115-116°C. <sup>1</sup>H-NMR (500 MHz, CDCl<sub>3</sub>):  $\delta$  7.71 (d, 1H,  $J$  = 8.6 Hz, H-2''), 7.53 – 7.44 (m, 1H, H-3), 7.43 (d, 2H,  $J$  = 8.7 Hz, H-2'', H-6''), 7.01 (d, 1H,  $J_{trans}$  = 15.0 Hz, H-2), 6.95 – 6.85 (m, 4H, H-4, H-5, H-3'', H-5''), 6.54 (dd, 1H,  $J$  = 8.6, 2.2 Hz, H-3'), 6.48 (d, 1H,  $J$  = 2.2 Hz, H-5'), 3.89 (s, 3H, H-7'), 3.86 (s, 3H, H-8'), 3.83 (s, 3H, H-7''). <sup>13</sup>C-NMR (126 MHz, CDCl<sub>3</sub>):  $\delta$  190.6 9 (C-1), 163.9 (C-4'), 160.2 (C-6'), 160.2 (C-4''), 143.1 (C-2), 140.5 (C-5), 132.7 (C-4), 129.5 (C-3), 129.2 (C-1''), 128.6 (C-2'', C-6''), 125.3 (C-1'), 122.3 (C-2'), 114.2 (C-3'', C-5''), 104.9 (C-3'), 98.5 (C-5'), 55.6 (C-7'), 55.5 (C-8'), 55.3 (C-7''). HRMS (ESI): m/z calcd for C<sub>20</sub>H<sub>20</sub>O<sub>4</sub>-H: 323.1109 [M-H]<sup>-</sup>; found: 323.1112.

**1-(2-Fluorophenyl)-5-(4-methoxyphenyl)penta-2,4-dien-1-one (3e)**

Yellow solid 57% yield; m.p. 90-91°C. <sup>1</sup>H-NMR (500 MHz, CDCl<sub>3</sub>):  $\delta$  7.78 (t, 1H,  $J$  = 7.5 Hz, H-2''), 7.57 – 7.48 (m, 2H, H-3, H-4'), 7.46 (d, 2H,  $J$  = 8.6 Hz, H-2'', H-6''), 7.25 (d, 1H,  $J$  = 7.5 Hz, H-4'), 7.16 (dd, 1H,  $J$  = 10.6, 8.5 Hz, H-4), 6.98 (d, 1H,  $J_{trans}$  = 15.5 Hz, H-2), 6.93 – 6.88 (m, 4H, H-3'', H-5''), H-5', H-5), 3.85 (s, 3H). <sup>13</sup>C-NMR (126 MHz, CDCl<sub>3</sub>):  $\delta$  189.4 (C-1), 160.6 (C-6'), 145.6 (C-4''), 142.2 (C-2), 130.8 (C-3), 130.8 (C-5), 128.9 (C-1'), 128.8 (C-2'', C-6''), 127.9 (C-1''), 127.8 (C-4), 124.7 (C-3'), 124.4 (C-3''), 124.4 (C-4'), 116.5 (C-2'), 116.3 (C-5'), 114.3 (C-3'', C-5''), 55.3 (C-7''). HRMS (ESI): m/z calcd for C<sub>18</sub>H<sub>15</sub>FO<sub>2</sub>-H: 281.1340 [M-H]<sup>-</sup>; found: 281.1337.

**1-(3-Fluorophenyl)-5-(4-methoxyphenyl)penta-2,4-dien-1-one (3f)**

Yellow solid 88% yield; m.p. 95-96°C. <sup>1</sup>H-NMR (500 MHz, CDCl<sub>3</sub>):  $\delta$  7.76 (d, 1H,  $J$  = 7.7 Hz, H-2''), 7.66 (d, 1H,  $J_{trans}$  = 15.1 Hz, H-2), 7.64 – 7.60 (m, 1H, H-3), 7.47-4.45 (m, 3H, H-2'', H-6'', H-5), 7.30 – 7.23 (m, 1H, H-3'), 7.02 (d, 1H,  $J$  = 5.9 Hz, H-6'), 6.99 (d, 1H,  $J$  = 5.3 Hz, H-4'), 6.94-6.91 (m, 3H, H-2'', H-5'', H-4), 3.85 (s, 3H, H-7''). <sup>13</sup>C-NMR (126 MHz, CDCl<sub>3</sub>):  $\delta$  189.1 (C-1), 163.8 (C-5'), 160.7 (C-4''), 146.1 (C-2), 142.4 (C-5), 130.1 (C-1'), 128.9 (C-2'', C-6''), 124.6 (C-1''), 123.6 (C-3), 119.5 (C-4), 119.3 (C-2'), 115.2 (C-3''), 114.3 (C-3'', C-5''), 55.3 (C-7''). HRMS (ESI): m/z calcd for C<sub>18</sub>H<sub>15</sub>FO<sub>2</sub>-H: 281.1339 [M-H]<sup>-</sup>; found: 281.1341.

**1-(4-Fluorophenyl)-5-(4-methoxyphenyl)penta-2,4-dien-1-one (3g)**

Yellow solid 55%; m.p. 130-131°C. <sup>1</sup>H-NMR (500 MHz, CDCl<sub>3</sub>):  $\delta$  8.02 (dd, 2H,  $J$  = 8.5, 5.6 Hz, H-2', H-6'), 7.62 (dd, 1H,  $J_{trans}$  = 14.8, 10.8 Hz, H-3), 7.47 (d, 2H,  $J$  = 8.6

Hz, H-3'', H-5''), 7.17 (t, 2H,  $J$  = 8.6 Hz, H-2'', H-6''), 7.06 – 6.97 (m, 2H, H-2, H-5), 6.95 – 6.88 (m, 3H, H-3'', H-5'', H-4), 3.86 (s, 3H, H-7''). <sup>13</sup>C-NMR (126 MHz, CDCl<sub>3</sub>):  $\delta$  188.8 (C-1), 166.5 (C-4'), 160.6 (C-4''), 145.6 (C-2), 142.1 (C-5), 130.9 (C-3), 130.8 (C-4), 128.9 (C-2', C-6'), 128.85 (C-3', C-5'), 124.6 (C-1'), 123.6 (C-1''), 115.7 (C-2'', C-6''), 114.3 (C-3'', C-5''), 55.3 (C-7''). HRMS (ESI): m/z calcd for C<sub>18</sub>H<sub>15</sub>FO<sub>2</sub>-H: 281.1341 [M-H]<sup>-</sup>; found: 281.1338.

**5-(4-Methoxyphenyl)-1-(5-methylthiophen-2-yl)penta-2,4-dien-1-one (3h)**

Yellowish orange solid 56%; m.p. 99-100°C. <sup>1</sup>H NMR (500 MHz, CDCl<sub>3</sub>):  $\delta$  7.61 – 7.55 (m, 2H, H-5', H-2), 7.44 (d, 2H,  $J$  = 8.6 Hz, H-2'', H-6''), 6.96 (d, 1H,  $J_{trans}$  = 15.5 Hz, H-2), 6.93 – 6.86 (m, 4H, H-3'', H-5'', H-4, H-5), 6.86 – 6.81 (m, 1H, H-4'), 3.84 (s, 3H, H-7''), 2.55 (s, 3H, H-6'). <sup>13</sup>C-NMR (126 MHz, CDCl<sub>3</sub>):  $\delta$  181.7 (C-1), 160.5 (C-4''), 149.6 (C-2), 143.9 (C-5), 143.6 (C-1'), 141.5 (C-4), 131.9 (C-1''), 128.9 (C-3), 128.7 (C-2'', C-6''), 126.8 (C-3'), 124.6 (C-4'), 123.7 (C-5'), 114.2 (C-3'', C-5''), 55.3 (C-7''), 16.1 (C-6'). HRMS (ESI): m/z calcd for C<sub>17</sub>H<sub>16</sub>O<sub>2</sub>S -H: 283.0089 [M-H]<sup>-</sup>; found: 283.0086.

**1-(Furan-2-yl)-5-(4-methoxyphenyl)penta-2,4-dien-1-one (3i)**

Yellow solid 88%; m.p. 116-117°C. <sup>1</sup>H-NMR (500 MHz, CDCl<sub>3</sub>):  $\delta$  7.70 – 7.65 (m, 1H, H-3), 7.63-7.62 (m, 2H, H-2', H-5'), 7.45 (d, 2H,  $J$  = 8.6 Hz, H-H-2'', H-6''), 6.99 (d, 2H,  $J_{trans}$  = 16.0 Hz, H-2, H-5), 6.95-6.86 (m, 3H, H-3'', H-5'', H-4), 6.59 – 6.55 (m, 1H, H-4'), 3.84 (s, 3H). <sup>13</sup>C-NMR (126 MHz, CDCl<sub>3</sub>):  $\delta$  178.1 (C-1), 160.6 (C-4''), 153.8 (C-2), 146.3 (C-5), 144.5 (C-3), 142.1 (C-1'), 128.9 (C-4), 128.8 (C-2'', C-6''), 124.6 (C-1''), 123.4 (C-4'), 117.0 (C-5'), 114.3 (C-3'', C-5''), 112.3 (C-3'), 55.3 (C-7''). HRMS (ESI): m/z calcd for C<sub>16</sub>H<sub>14</sub>O<sub>3</sub>-H: 253.0419 [M-H]<sup>-</sup>; found: 253.0421.

**1-(2-Fluoro-4-methoxyphenyl)-5-(4-methoxyphenyl)penta-2,4-dien-1-one (3j)**

Yellow solid 64% yield; m.p. 117-118°C. <sup>1</sup>H-NMR (500 MHz, CDCl<sub>3</sub>):  $\delta$  7.85 (t, 1H,  $J$  = 8.7 Hz, H-2''), 7.56 (dd, 1H,  $J_{trans}$  = 13.3, 11.6 Hz, H-3), 7.44 (d, 2H,  $J$  = 8.5 Hz, H-2'', H-6''), 6.99 – 6.96 (m, 1H, H-5'), 6.96 – 6.92 (m, 1H, H-3'), 6.89 – 6.84 (m, 3H, H-3'', H-5'', H-2), 6.79 – 6.74 (m, 1H, H-5), 6.63 (dd, 1H,  $J_{trans}$  = 12.9, 1.5 Hz, H-4), 3.85 (s, 3H), 3.82 (s, 3H). <sup>13</sup>C-NMR (126 MHz, CDCl<sub>3</sub>):  $\delta$  187.1 (C-1), 160.5 (C-6'), 144.6 (C-4'), 141.6 (C-4''), 132.5 (C-2), 132.5 (C-5), 129.0 (C-3), 128.8 (C-1'), 127.8 (C-2'', C-6''), 127.8 (C-1''), 125.0 (C-4), 114.2 (C-3'', C-5''), 110.6 (C-3'), 110.6 (C-5'), 101.8 (C-2'), 55.8 (C-7'), 55.3 (C-7''). HRMS (ESI): m/z calcd for C<sub>19</sub>H<sub>17</sub>FO<sub>3</sub>-H: 311.1110 [M-H]<sup>-</sup>; found: 311.1113.

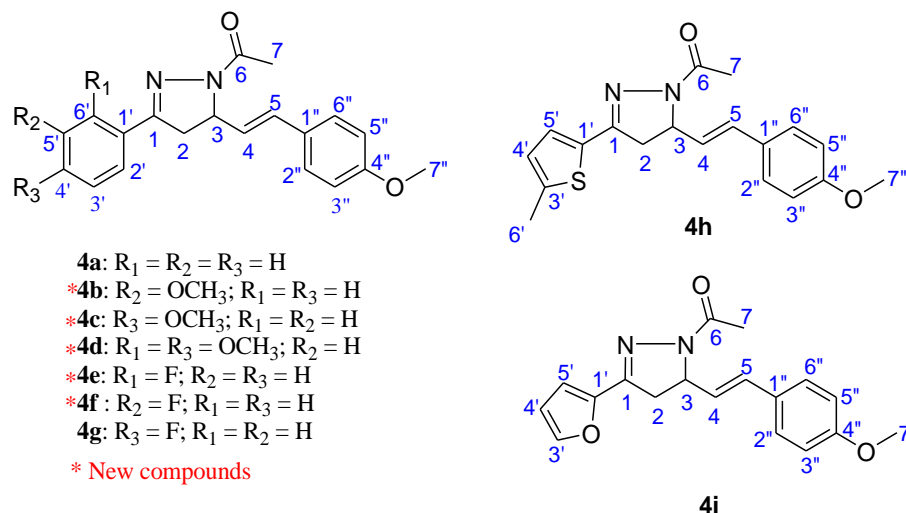


**Figure 3.** Chemical structures of series 4

### General Procedure for the Synthesis of Series 4

Consequently, a mixture of diarylpentadienone (**3a-j**, 1mmol), hydrazine hydrate (15 mmol), and glacial acetic acid (100%) was refluxed for three hours and then quenched with crushed ice. The crude mixture was first extracted with ethyl acetate ( $3 \times 20$  mL), dried over anhydrous  $MgSO_4$ , concentrated in vacuo to afford the crude products, and subjected to column chromatography using the hexane and ethyl acetate solvent system to afford the desired pyrazoline derivatives **4a-i** [28, 29]. The numbering of the carbons/hydrogens in the series **4** structure used in the structural NMR analysis is shown in Figure 3.

#### *1-(5-(4-Methoxystyryl)-3-phenyl-4,5-dihydro-1H-pyrazol-1-yl)ethanone (4a)*

White solid 9%; m.p. 99-100°C. FT-IR (ATR): 1659.78 (C=N), 1649.14 (C=O), 1415.75 (C=C), 1244.09 (C-O)  $cm^{-1}$ .  $^1H$ -NMR (500 MHz,  $CDCl_3$ ):  $\delta$  7.77 – 7.71 (m, 2H, H-2', H-6'), 7.45 – 7.41 (m, 3H, H-3', H-4', H-5'), 7.29 (d, 2H,  $J = 8.6$  Hz, H-2'', H-6''), 6.81 (d, 2H,  $J = 8.6$  Hz, H-3'', H-5''), 6.55 (d, 1H,  $J_{trans} = 15.8$  Hz, H-5), 6.07 (dd, 1H,  $J_{trans} = 15.9, 7.1$  Hz, H-4), 5.35 – 5.20 (m, 1H, H-3), 3.79 (s, 3H, H-7''), 3.54 (dd, 1H,  $J = 17.5, 11.3$  Hz, H-2), 3.12 (dd, 1H,  $J = 17.5, 4.2$  Hz, H-2), 2.42 (s, 3H, H-7).  $^{13}C$ -NMR (126 MHz,  $CDCl_3$ ):  $\delta$  168.9 (C-6), 159.5 (C-4''), 154.3 (C-1), 131.5 (C-1'), 130.9 (C-5), 130.2 (C-1''), 128.9 (C-4), 128.7 (C-2', C-6'), 127.8 (C-3', C-5'), 126.5 (C-2'', C-6''), 124.8 (C-4'), 113.8 (C-3'', C-5''), 58.0 (C-3), 55.2 (C-7''), 39.4 (C-2), 22.1 (C-7). HRMS (ESI):  $m/z$  calcd for  $C_{20}H_{20}N_2O_2 \cdot H$ : 319.0019 [M-H]<sup>-</sup>; found: 319.0021.

#### *1-(3-(3-Methoxyphenyl)-5-(4-methoxystyryl)-4,5-dihydro-1H-pyrazol-1-yl)ethanone (4b)*

White solid 17% yield; m.p. 108-109°C. FT-IR (ATR):

1643.35 (C=N), 1606.70 (C=O), 1425.40 (C=C), 1240.23 (C-O)  $cm^{-1}$ .  $^1H$ -NMR (500 MHz,  $CDCl_3$ ):  $\delta$  7.35 (d, 1H,  $J = 7.9$  Hz, H-6'), 7.32 (d, 1H,  $J = 5.5$  Hz, H-2'), 7.29 (d, 2H,  $J = 8.6$  Hz, H-2'', H-6''), 6.98 (dd, 1H,  $J = 8.1, 2.3$  Hz, H-3'), 6.81 (d, 2H,  $J = 8.6$  Hz, H-3'', H-5''), 6.54 (d, 1H,  $J_{trans} = 15.8$  Hz, H-5), 6.06 (dd, 1H,  $J_{trans} = 15.8, 7.1$  Hz, H-4), 5.30 – 5.22 (m, 1H, H-3), 3.86 (s, 3H, H-7'), 3.79 (s, 3H, H-7''), 3.52 (dd, 1H,  $J = 17.5, 11.3$  Hz, H-2), 3.10 (dd, 1H,  $J = 17.5, 4.3$  Hz, H-2), 2.41 (s, 3H, H-7).  $^{13}C$ -NMR (126 MHz,  $CDCl_3$ ):  $\delta$  169.1 (C-6), 159.7 (C-5'), 159.3 (C-4''), 154.0 (C-1), 132.8 (C-1'), 130.9 (C-5), 129.7 (C-1''), 128.9 (C-2'', C-6''), 127.8 (C-6'), 124.8 (C-2'), 119.1 (C-4'), 116.0 (C-4), 113.8 (C-3'', C-5''), 111.4 (C-3'), 58.0 (C-3), 55.3 (C-7'), 55.2 (C-7''), 39.4 (C-2), 22.1 (C-7). HRMS (ESI):  $m/z$  calcd for  $C_{21}H_{22}N_2O_3 \cdot H$ : 349.4091 [M-H]<sup>-</sup>; found: 349.4088.

#### *1-(3-(4-Methoxyphenyl)-5-(4-methoxystyryl)-4,5-dihydro-1H-pyrazol-1-yl)ethanone (4c)*

Light yellow solid 13% yield; m.p. 107-108°C. FT-IR (ATR): 1660.71 (C=N), 1649.14 (C=O), 1413.82 (C=C), 1244 (C-O)  $cm^{-1}$ .  $^1H$ -NMR (500 MHz,  $CDCl_3$ ):  $\delta$  7.68 (d, 2H,  $J = 8.6$  Hz, H-2', H-6'), 7.29 (d, 2H,  $J = 8.5$  Hz, H-3', H-5'), 6.94 (d, 2H,  $J = 8.6$  Hz, H-2'', H-6''), 6.81 (d, 2H,  $J = 8.5$  Hz, H-3'', H-5''), 6.53 (d, 1H,  $J_{trans} = 15.8$  Hz, H-5), 6.06 (dd, 1H,  $J_{trans} = 15.8, 7.0$  Hz, H-4), 5.30 – 5.14 (m, 1H, H-3), 3.85 (s, 3H, H-7'), 3.78 (s, 3H, H-7''), 3.50 (dd, 1H,  $J = 17.3, 11.3$  Hz, H-2), 3.08 (dd, 1H,  $J = 17.4, 3.9$  Hz, H-2), 2.40 (s, 3H, H-7).  $^{13}C$ -NMR (126 MHz,  $CDCl_3$ ):  $\delta$  168.8 (C-6), 161.2 (C-4'), 159.3 (C-4''), 153.9 (C-1), 130.7 (C-1'), 129.0 (C-5), 128.0 (C-2', C-6'), 127.8 (C-3', C-5'), 125.0 (C-1''), 124.1 (C-4), 114.1 (C-3'', C-6''), 113.84 (C-3'', C-5''), 57.8 (C-3), 55.3 (C-7'), 55.2 (C-7''), 39.5 (C-2), 22.0 (C-7). HRMS (ESI):  $m/z$  calcd for  $C_{21}H_{22}N_2O_3 \cdot H$ : 349.4090 [M-H]<sup>-</sup>; found: 349.4092.

**1-(3-(2,4-Dimethoxyphenyl)-5-(4-methoxystyryl)-4,5-dihydro-1H-pyrazol-1-yl)ethanone (4d)**

Light yellow solid 6% yield; m.p. 91-92°C. FT-IR (ATR): 1651.07 (C=N), 1604.77 (C=O), 1406.11 (C=C), 1244.09 (C-O)  $\text{cm}^{-1}$ .  $^1\text{H-NMR}$  (500 MHz,  $\text{CDCl}_3$ ):  $\delta$  7.83 (d, 1H,  $J = 8.7$  Hz, H-2'), 7.28 (d, 2H,  $J = 8.6$  Hz, H-2'', H-6''), 6.80 (d, 2H,  $J = 8.6$  Hz, H-3'', H-5''), 6.53 (d, 1H,  $J = 8.6$  Hz, H-5'), 6.48 (d, 2H,  $J = 18.1$  Hz, H-5, H-3'), 6.06 (dd, 1H,  $J_{\text{trans}} = 15.8, 7.0$  Hz, H-4), 5.22 – 5.10 (m, 1H, H-3), 3.83 (s, 3H, H-7'), 3.82 (s, 3H, H-8'), 3.77 (s, 3H, H-7''), 3.60 (dd, 1H,  $J = 18.3, 11.2$  Hz, H-2), 3.24 (dd, 1H,  $J = 18.3, 4.1$  Hz, H-2), 2.38 (s, 3H, H-7).  $^{13}\text{C-NMR}$  (126 MHz,  $\text{CDCl}_3$ ):  $\delta$  168.8 (C-6), 162.5 (C-6'), 159.5 (C-4'), 159.1 (C-4''), 154.3 (C-1), 130.3 (C-1'), 130.0 (C-5), 129.2 (C-1''), 127.7 (C-2'', C-6''), 125.4 (C-2'), 113.8 (C-5'), 113.6 (C-3'', C-5''), 105.4 (C-4), 98.5 (C-3'), 57.7 (C-3), 55.5 (C-7'), 55.4 (C-8'), 55.2 (C-7''), 42.5 (C-2), 22.1 (C-7). HRMS (ESI):  $m/z$  calcd for  $\text{C}_{22}\text{H}_{24}\text{N}_2\text{O}_4\text{-H}$ : 379.1907 [M-H] $^-$ ; found: 379.1906.

**1-(3-(2-Fluorophenyl)-5-(4-methoxystyryl)-4,5-dihydro-1H-pyrazol-1-yl)ethanone (4e)**

Light yellow solid 52% yield; m.p. 95-96°C. FT-IR (ATR): 1649.70 (C=N), 1606.14 (C=O), 1408.04 (C=C), 1229.87 (C-O)  $\text{cm}^{-1}$ .  $^1\text{H-NMR}$  (500 MHz,  $\text{CDCl}_3$ ):  $\delta$  7.95 (t, 1H,  $J = 7.7$  Hz, H-2'), 7.40 (dd, 1H,  $J = 13.3, 6.8$  Hz, H-3'), 7.30 (d, 2H,  $J = 8.5$  Hz, H-2'', H-6''), 7.20 (t, 1H,  $J = 7.6$  Hz, H-4'), 7.12 - 7.11 (m, 1H, H-5'), 6.82 (d, 2H,  $J = 8.5$  Hz, H-3'', H-5''), 6.54 (d, 1H,  $J_{\text{trans}} = 15.8$  Hz, H-5), 6.07 (dd, 1H,  $J_{\text{trans}} = 15.8, 7.0$  Hz, H-4), 5.33 – 5.20 (m, 1H, H-3), 3.79 (s, 3H, 7''), 3.69 – 3.60 (m, 1H, H-2), 3.28 – 3.20 (m, 1H, H-2), 2.41 (s, 3H, H-7).  $^{13}\text{C-NMR}$  (126 MHz,  $\text{CDCl}_3$ ):  $\delta$  169.1 (C-6), 162.1 (C-6'), 160.1 (C-4''), 159.3 (C-1), 151.0 (C-1'), 131.8 (C-5), 130.8 (C-1''), 128.9 (C-2'), 128.7 (C-4'), 127.8 (C-2'', C-6''), 124.8 (C-3'), 124.4 (C-5'), 116.6 (C-4), 113.8 (C-3'', C-5''), 58.0 (C-3), 55.2 (C-7''), 41.7 (C-2), 22.1 (C-7). HRMS (ESI):  $m/z$  calcd for  $\text{C}_{20}\text{H}_{19}\text{FN}_2\text{O}_2\text{-H}$ : 337.1019 [M-H] $^-$ ; found: 337.1018.

**1-(3-(3-Fluorophenyl)-5-(4-methoxystyryl)-4,5-dihydro-1H-pyrazol-1-yl)ethanone (4f)**

Cream white solid 42% yield; m.p. 115-116°C. FT-IR (ATR): 1649.14 (C=N), 1606.70 (C=O), 1408.04 (C=C), 1249.87 (C-O)  $\text{cm}^{-1}$ .  $^1\text{H-NMR}$  (500 MHz,  $\text{CDCl}_3$ ):  $\delta$  7.53 – 7.45 (m, 2H, H-2', H-6'), 7.42-7.37 (m, 1H, H-3'), 7.29 (d, 2H,  $J = 8.6$  Hz, H-2'', H-6''), 7.12-7.11 (m, 1H, H-4), 6.82 (d, 2H,  $J = 8.6$  Hz, H-3'', H-5''), 6.54 (d, 1H,  $J_{\text{trans}} = 15.8$  Hz, H-5), 6.06 (dd, 1H,  $J_{\text{trans}} = 15.8, 7.1$  Hz, H-4), 5.32 – 5.24 (m, 1H, H-3), 3.79 (s, 3H, H-7'), 3.52 (dd, 1H,  $J = 17.4, 11.3$  Hz, H-2), 3.08 (dd, 1H,  $J = 17.5, 4.4$  Hz, H-2), 2.41 (s, 3H, H-7).  $^{13}\text{C-NMR}$  (126 MHz,  $\text{CDCl}_3$ ):  $\delta$  169.1 (C-6), 163.8

(C-5'), 161.8 (C-3'), 159.3 (C-4''), 152.9 (C-1), 133.7 (C-1'), 131.1 (C-5), 128.8 (C-1''), 127.8 (C-2'', C-6''), 124.6 (C-4), 122.3 (C-2'), 115.1 (C-4), 113.4 (C-3'', C-5'') 113.0 (C-6'), 58.2 (C-3), 55.2 (C-7''), 39.3 (C-2), 22.1 (C-7). HRMS (ESI):  $m/z$  calcd for  $\text{C}_{20}\text{H}_{19}\text{FN}_2\text{O}_2\text{-H}$ : 337.1021 [M-H] $^-$ ; found: 337.1018.

**1-(3-(4-Fluorophenyl)-5-(4-methoxystyryl)-4,5-dihydro-1H-pyrazol-1-yl)ethanone (4g)**

White solid 12%; m.p. 104-105°C. FT-IR (ATR): 1647.21 (C=N), 1602.85 (C=O), 1408.04 (C=C), 1226.73 (C-O)  $\text{cm}^{-1}$ .  $^1\text{H-NMR}$  (500 MHz,  $\text{CDCl}_3$ ):  $\delta$  7.73 (dd, 2H,  $J = 8.6, 5.4$  Hz, H-2', H-6'), 7.29 (d, 2H,  $J = 8.6$  Hz, H-3', H-5'), 7.12 (t, 2H,  $J = 8.6$  Hz, H-2'', H-6''), 6.82 (d, 2H,  $J = 8.6$  Hz, H-3'', H-5''), 6.54 (d, 1H,  $J_{\text{trans}} = 15.8$  Hz, H-5), 6.06 (dd, 1H,  $J_{\text{trans}} = 15.8, 7.1$  Hz, H-4), 5.33 – 5.22 (m, 1H, H-3), 3.79 (s, 3H, H-7''), 3.52 (dd, 1H,  $J = 17.4, 11.3$  Hz, H-2), 3.08 (dd, 1H,  $J = 17.4, 4.4$  Hz, H-2), 2.40 (s, 3H, H-7).  $^{13}\text{C-NMR}$  (126 MHz,  $\text{CDCl}_3$ ):  $\delta$  169.0 (C-6), 159.3 (C-4'), 153.0 (C-1), 130.9 (C-4''), 128.8 (C-1'), 128.5 (C-1''), 128.4 (C-2', C-6'), 127.8 (C-3', C-5'), 124.7 (C-4), 115.7 (C-2'', C-6''), 113.87 (C-3'', C-5''), 58.1 (C-3), 55.2 (C-7''), 39.4 (C-2), 22.1 (C-7). HRMS (ESI):  $m/z$  calcd for  $\text{C}_{20}\text{H}_{19}\text{FN}_2\text{O}_2\text{-H}$ : 337.1020 [M-H] $^-$ ; found: 337.1017.

**1-(5-(4-Methoxystyryl)-3-(5-methylthiophen-2-yl)-4,5-dihydro-1H-pyrazol-1-yl)ethanone (4h)**

Light yellow solid 15%; m.p. 117-118°C. FT-IR (ATR): 1658.78 (C=N), 1645.28 (C=O), 1415.75 (C=C), 1244.09 (C-O)  $\text{cm}^{-1}$ .  $^1\text{H-NMR}$  (500 MHz,  $\text{CDCl}_3$ ):  $\delta$  7.29 (d, 2H,  $J = 8.6$  Hz, H-2'', H-6''), 7.03 (d, 1H,  $J = 3.5$  Hz, H-5), 6.81 (d, 2H,  $J = 8.7$  Hz, H-3'', H-5''), 6.72 (d, 1H,  $J = 2.5$  Hz, H-4'), 6.53 (d, 1H,  $J_{\text{trans}} = 15.8$  Hz, H-5), 6.05 (dd, 1H,  $J_{\text{trans}} = 15.8, 7.1$  Hz, H-4), 5.33 – 5.15 (m, 1H, H-3), 3.79 (s, 3H, H-7''), 3.49 (dd, 1H,  $J = 17.1, 11.3$  Hz, H-2), 3.05 (dd, 1H,  $J = 17.2, 4.2$  Hz, H-2), 2.52 (s, 3H, H-6'), 2.36 (s, 3H, H-7).  $^{13}\text{C-NMR}$  (126 MHz,  $\text{CDCl}_3$ ):  $\delta$  168.8 (C-6), 159.2 (C-4''), 150.0 (C-1), 143.9 (C-1'), 132.8 (C-5), 132.7 (C-1''), 130.9 (C-3'), 128.9 (C-4'), 127.8 (C-2'', C-6''), 125.8 (C-5'), 124.7 (C-4), 113.8 (C-3'', C-5''), 58.0 (C-3), 55.2 (C-7''), 39.9 (C-2), 22.0 (C-7), 15.6 (C-6'). HRMS (ESI):  $m/z$  calcd for  $\text{C}_{19}\text{H}_{20}\text{N}_2\text{O}_2\text{S-H}$ : 339.0033 [M-H] $^-$ ; found: 339.0031.

**1-(3-(Furan-2-yl)-5-(4-methoxystyryl)-4,5-dihydro-1H-pyrazol-1-yl)ethanone (4i)**

Cream white solid 22% yield; m.p. 123-124°C. FT-IR (ATR): 1645.28 (C=N), 1606.70 (C=O), 144.61 (C=C), 1242.16 (C-O)  $\text{cm}^{-1}$ .  $^1\text{H-NMR}$  (500 MHz,  $\text{CDCl}_3$ ):  $\delta$  7.55 (s, 1H, H-5'), 7.28 (d, 2H,  $J = 8.5$  Hz, 2H, H-2'', H-6''), 6.81 (d, 2H,  $J = 8.6$  Hz, H-3'', H-5''), 6.75 (d, 1H,  $J = 3.3$  Hz, 1H, H-3'), 6.53 (d, 2H,  $J_{\text{trans}} = 16.0$  Hz, H-4', H-5), 6.04 (dd, 1H,  $J_{\text{trans}} = 15.8, 7.0$  Hz, H-4),

5.29 – 5.22 (m, 1H, H-3), 3.78 (s, 3H, H-7''), 3.47 (dd, 1H,  $J = 17.4, 11.3$  Hz, H-2), 3.04 (dd, 1H,  $J = 17.4, 4.2$  Hz, H-2), 2.39 (s, 3H, H-7).  $^{13}\text{C}$ -NMR (126 MHz,  $\text{CDCl}_3$ ):  $\delta$  169.0 (C-6), 159.38 (C-4''), 146.9 (C-1), 145.9 (C-1'), 144.6 (C-3'), 131.0 (C-5), 128.8 (C-1''), 127.8 (C-2'', C-6''), 124.4 (C-4), 113.8 (C-3'', C-5''), 112.5 (C-4'), 111.9 (C-5'), 57.6 (C-3), 55.2 (C-7''), 39.1 (C-2), 22.1 (C-7). HRMS (ESI):  $m/z$  calcd for  $\text{C}_{18}\text{H}_{18}\text{N}_2\text{O}_3\text{-H}$ : 309.1100 [M-H] $^-$ ; found: 309.1098.

### ***In silico* Pan-Assay Interference Compounds (PAINS) and Aggregator Identification**

All designed and synthesized chemical structures were first drawn using ChemDraw Ultra 12.0, converted to SMILES and Symyx SDF (Spatial Data File) file format as suggested by FAF-Drugs4 Bank Formatter (<http://mobyli.e.rpbs.univ-paris-diderot.fr/cgi-bin/portal.py#forms::Bank-Formatter>). Filtering of PAINS was performed using PAINS Filter A, B, and C via the FAF-Drugs4 Server (<http://mobyli.e.rpbs.univ-paris-diderot.fr/cgi-bin/portal.py#forms::FAF-Drugs4>) [30]. The generated results are available at the following address: <https://mobyli.e.rpbs.univ-paris-diderot.fr/cgi-bin/portal.py#jobs::FAF-Drugs4.Y01828762082100>. Meanwhile, the SMILES file containing the synthesized diarylpentadienones and their pyrazoline derivatives generated from the *in silico* PAINS analysis was submitted to the Aggregator Advisor Server (<http://advisor.bkslab.org/>) for identification of potential aggregators [31].

### **Biological Assays**

#### **$\alpha$ -Glucosidase Inhibitory Assay**

$\alpha$ -Glucosidase inhibition experiment was performed using a modified version of a previously established method [32].  $\alpha$ -Glucosidase originated from yeast maltase was used as the enzyme source, while the respective *p*-nitrophenyl- $\alpha$ -D-glucopyranoside (PNPG) and acarbose were used as substrate and positive control in this assay. All compounds were prepared for the screening assay at a concentration of 50  $\mu\text{M}$  (known as pre-centrifugation sample). A mixture of 10  $\mu\text{L}$  of the tested sample, 130  $\mu\text{L}$  of phosphate buffer (pH 6.5, 30 mM) and 10  $\mu\text{L}$  of enzyme in a 96-well plate was pre-incubated for 5 minutes at room temperature. On a side note, the post-centrifugation sample was prepared by centrifuging the tested compounds (at a concentration of 50  $\mu\text{M}$ ) at approximately 15,000 g for 30 minutes at 4  $^\circ\text{C}$ , following the aggregation assay method by Auld et al. (2017) [33, 34]. Potential aggregates were expected to form a sediment while the resulting supernatant was separated and used for testing. This is important to study the aggregation of the assayed compound using

the centrifugation counter-screen technique by comparing the biological activity between the samples before and after centrifugation [33]. Next, 50  $\mu\text{L}$  of PNPG substrate solution (10 mM) was added and the mixture was further incubated for 15 minutes. The reaction was then quenched after pipetting 50  $\mu\text{L}$  of 2M glycine (pH 10) into the mixture, and the absorbance of the released *p*-nitrophenol was determined at 405 nm using a Tecan Safire spectrophotometer (Groedig, Austria). Subsequently,  $\text{IC}_{50}$  measurements (> 50%  $\alpha$ -glucosidase suppression) were performed in serial dilutions of the assayed compounds (400 to 6.25  $\mu\text{M}$ ), analyzed with a nonlinear regression method using GraphPad Prism (version 7.0; GraphPad software), and expressed as mean  $\pm$  SEM. All assays were performed in triplicate wells and repeated three times.

#### **DPPH Free Radical Scavenging Assay**

DPPH radical scavenging was performed by the method of Wan et al. (2012) [35], using quercetin as a positive control. Each 96-well microplate was filled with 100  $\mu\text{L}$  of 1000  $\mu\text{g}/\text{mL}$  of the tested samples and 100  $\mu\text{L}$  of DPPH (19.7 mg/250 mL), incubated in the dark for 30 minutes, and the absorbance was measured at 515 nm using a Tecan Safire spectrometer (Groedig, Austria). The scavenging capacity of the samples was determined using the formula  $\text{SC}\% = [(A_0 - A_s) / A_0] \times 100$ , where  $A_0$  and  $A_s$  are the absorbance of the reagent blank values and the tested samples, respectively. For each sample, the analysis was performed in triplicate.  $\text{IC}_{50}$  determination (> 50% DPPH scavenging) was performed with serial dilutions of the tested molecules, calculated with nonlinear regression via GraphPad Prism (version 7.0 GraphPad software) and expressed as mean ( $\mu\text{g}/\text{mL}$ )  $\pm$  SEM, followed by conversion to mean ( $\mu\text{M}$ )  $\pm$  SEM [35].

#### **Nitric Oxide Scavenging Assay**

The nitric oxide (NO) scavenging assay was performed following Abd Ghafar et al. (2018) [36] with slight modifications. First, 60  $\mu\text{L}$  of 10 mM sodium nitroprusside (SNP) in PBS was mixed with 60  $\mu\text{L}$  of a concentration of 1000  $\mu\text{g}/\text{mL}$  of the tested samples and then incubated for 180 min at 25 $^\circ\text{C}$  in the presence of light. Griess reagent (60  $\mu\text{L}$ ) was then added to each well to measure the concentration of accumulated nitrites before quantification of absorbance using a Tecan Safire spectrophotometer (Groedig, Austria) at 550 nm.  $\text{IC}_{50}$  measurements (> 50% inhibition) were performed using serial dilution of the selected samples, calculated using GraphPad Prism (version 7.0; GraphPad software), and expressed as mean ( $\mu\text{g}/\text{mL}$ )  $\pm$  SEM followed by conversion to mean ( $\mu\text{M}$ )  $\pm$  SEM. Quercetin and gallic acid were used as positive controls in this experiment [36].

## Molecular Docking

AutoDock tools 1.5.6 (ADT) and AutoDock Vina 1.1.2 were employed for molecular docking experiments.

## Receptor Preparation

The Protein Data Bank (<https://www.rcsb.org/>) and the Uniprot database ([www.uniprot.org](http://www.uniprot.org)) were used to find the respective crystal structures of isomaltase (PDB ID: 3A4A) and the wild-type protein of human peroxiredoxin with bound DTT as a competitive inhibitor (PDB ID: 3MNG) and the  $\alpha$ -glucosidase sequence (P53341) of *Saccharomyces cerevisiae*. Alignment of the P53341 sequence of 3A4A was performed via Discovery Studio 2.5, followed by creation of the homology model of  $\alpha$ -glucosidase based on the generated sequence template in the MODELER program of Discovery Studio 2.5. The model with the lowest modeler objective function was selected for Ramachandran plot validation obtained from the RAMPAGE server before molecular docking was performed [37]. Next, ADT was applied to insert polar hydrogens and Gasteiger charges into all proteins studied, and the resulting receptors were saved in PDBQT format.

## Ligands Preparation

The 3D structures of compounds **3d**, **3h**, **4f**, acarbose, DTT, and quercetin were prepared using Chem Office software, energy minimized, and saved in PDB format. Then, the polar hydrogens and Gasteiger charges in all tested compounds were added by ADT and the generated structures were subsequently saved in PDBQT format.

## Docking with Autodock Vina

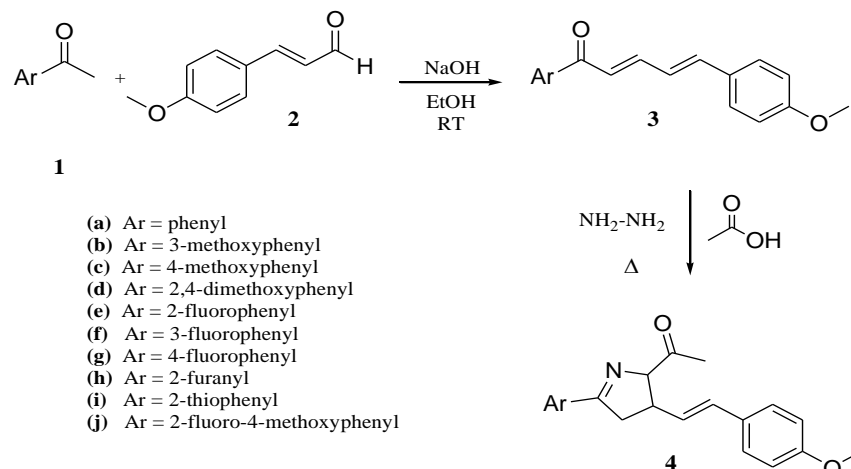
AutoDock Vina was used for molecular docking of the bioactive compounds to the homology-modeled  $\alpha$ -glucosidase and peroxiredoxin crystals. The coordinates

of the ligand binding domain were retrieved from the literature. The 3D and 2D protein-ligand interactions were analyzed using Accelrys Discovery Studio Visualizer v4.1.0.14169 (San Diego, USA) [38].

## RESULTS AND DISCUSSION

### Chemistry

In the present study, the *trans* diarylpentadienones (compounds **3**) were successfully synthesized via a base-catalyzed Claisen-Schmidt condensation reaction by treating **a-j** various acetophenones (**1**) and 4-methoxycinnamaldehyde (**2**), as shown in Scheme 1 [27]. The mixture was further purified via the gravitational column chromatography and the isolated pure compound was analyzed by  $^1\text{H-NMR}$  and  $^{13}\text{C-NMR}$  for preliminary structure confirmation. The analogues containing an electron donating group at the *ortho*- and *para*- positions of the aromatic ring A improved the product yield up to 91%, while lower product percentages (55-62%) were obtained with the electron withdrawing-substituted compounds. As for the heterocyclic analogues, a high yield was observed with a higher electron density furanyl-containing analogue (89%) compared to the 5-methylthiophenyl-containing diarylpentadienone (56% yield). Subsequently, the new pyrazoline derivatives (**4a-i**) except **4a**, **4g** and **4h**, were prepared by condensation of the corresponding **3a-j** with hydrazine hydrate in glacial acetic acid under reflux conditions for 3 hours. The crude products of all compounds were purified by column chromatography, with yields ranging from 6-52%, and were characterized spectroscopically via  $^1\text{H-}$  and  $^{13}\text{C-NMR}$ , FT-IR, and high-resolution mass spectrometry (HRMS). All structural characterization and physical data, as well as  $^1\text{H-}$  and  $^{13}\text{C-NMR}$  data, are listed and summarized in Table S1 and Figure S1.1 to S1.20 in the Supplementary Material, respectively.



**Scheme 1.** General synthesis of diarylpentadienones **3** and pyrazole derivatives **4** (Adapted from [27])



### ***In silico* Pan-Assay Interference Compounds (PAINS) and Aggregator Identification**

In recent years, there have been controversial debates about the proclivity of tiny bioactive molecules as potential new drugs [39, 40, 41, 42]. Molecules with reactive structure functionality, known as PAINS, often contribute to false-positive bioactivity profiles and are regularly associated with nonspecific binding and assay interference. Therefore, we subjected all 19 designed diarylpentadienones and their new pyrazoline derivatives to the public electronic filters, FAF-Drugs4 and Aggregator Advisor [43], to detect PAINS and aggregators, respectively.

According to the PAINS filtration results (Figure S2 of Supplementary Material), none of the designed compounds were PAINS-related and aggregator-related molecules. However, with a reasonably high estimated LogP (3.0 to 4.6), all the studied molecules, compounds **3a-j** and **4a-i**, were predicted to be potential aggregates. It was noted that many identified aggregators had previously exhibited LogP ranges of  $> 3.0$  [44]. Hence, we examined the aggregation of the most significant  $\alpha$ -glucosidase inhibitor **3h** (*in vitro* results will be discussed in the next Section) via the centrifugation counter-screen technique [33] to validate the prediction. Theoretically, this process causes the formation of pellets from aggregates, leaving only the monomeric compound in the supernatant after centrifugation, resulting in lower bioactivity compared to the tested pre-centrifuged analogues. [34, 43, 45]. As shown in Figure 4, the pre-

and post-centrifugal supernatants of **3h** were comparable in terms of  $\alpha$ -glucosidase suppression activities, with  $IC_{50}$   $40.52 \pm 2.0 \mu\text{M}$  and  $45 \pm 2.8 \mu\text{M}$ , respectively. These recorded results confirmed that the  $\alpha$ -glucosidase inhibitory activity of **3h** was not due to aggregate formation.

The physicochemical properties of all nineteen synthesized molecules were also predicted using the FAF-Drugs4 server in-silico and are summarized in Table 1. The results indicate that all molecules conformed to Lipinski's rule of five (RO5) with relatively significant 'lead-like' characteristics, according to Veber's rules. All compounds exhibited physicochemical properties within a defined range, including a molecular weight of less than 500 Da, less than five hydrogen bond donor groups, no more than ten hydrogen bond acceptor groups, and a calculated partition coefficient between n-octanol and water of no more than five (measuring lipophilicity) [43]. Veber et al. (2002) [46] concluded that the molecular flexibility and polar surface area of a molecule play an important role in the oral bioavailability of a drug, which led to the use of additional parameters, including total polar surface area of less than  $140 \text{ \AA}^2$  ( $TPSA \leq 140$ ) and no more than 10 rotatable bonds ( $NRB \leq 10$ ) [40]. Accordingly, FAF drugs4 predicted good bioavailability for all synthesized molecules. They complied with both VEBER (good oral bioavailability if  $NRB \leq 10$   $TPSA \leq 140 \text{ \AA}^2$ ) and EGAN rules (good oral bioavailability if  $-1 \leq \log P \leq 5.8$  and  $TPSA \leq 130 \text{ \AA}^2$ ) [47].

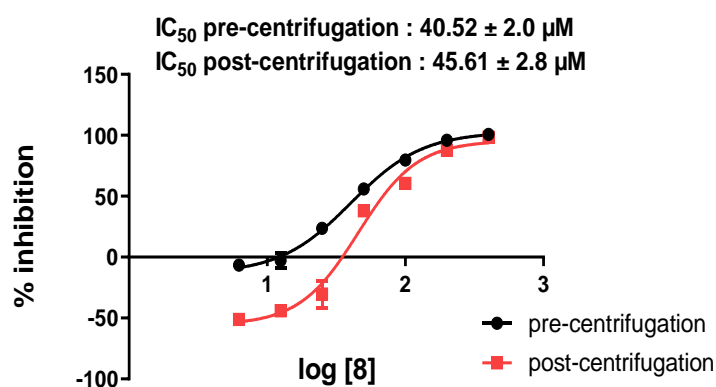
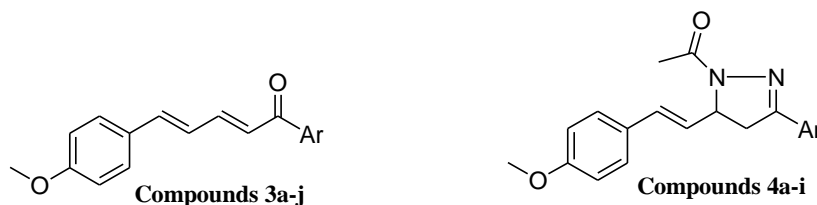


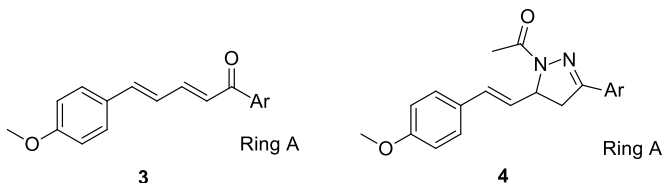
**Figure 4.** Dose-response curves of **3h** in confirming aggregate formation by the centrifugation counter-screen method

**Table 1.** Physicochemical and drug likeness properties of compounds calculated via FAF-Drugs4



Compound	Ar	MW (g/mol)	HB D	HB A	Lo g P	TPS A (Å <sup>2</sup> )	NR B	Oral bioavailabilit y (VEBER)	Oral bioavailabilit y (EGEN)
<b>3a</b>	Phenyl	264.32	0	2	4.4	26.30	5	Good	Good
<b>3b</b>	3- methoxyphenyl	294.34	0	3	4.4	35.53	6	Good	Good
<b>3c</b>	4- methoxyphenyl	294.34	0	3	4.4	35.53	6	Good	Good
<b>3d</b>	2,4- dimethoxypheny l	324.37	0	4	4.4	44.76	7	Good	Good
<b>3e</b>	2-fluorophenyl	282.31	0	2	4.5	26.30	5	Good	Good
<b>3f</b>	3-fluorophenyl	282.31	0	2	4.5	26.30	5	Good	Good
<b>3g</b>	4-fluorophenyl	282.31	0	2	4.6	26.30	5	Good	Good
<b>3h</b>	5- methylthiophen- 2-yl	284.37	0	2	4.5	54.54	5	Good	Good
<b>3i</b>	furan-2-yl	254.28	0	3	3.6	39.44	5	Good	Good
<b>3j</b>	2-fluoro-4- methoxyphenyl	312.33	0	3	4.5	35.53	6	Good	Good
<b>4a</b>	Phenyl	320.39	0	4	3.7	41.90	4	Good	Good
<b>4b</b>	3- methoxyphenyl	350.41	0	5	3.8	51.13	5	Good	Good
<b>4c</b>	4- methoxyphenyl	350.41	0	5	3.8	51.13	5	Good	Good
<b>4d</b>	2,4- dimethoxypheny l	380.44	0	6	3.8	60.36	6	Good	Good
<b>4e</b>	2-fluorophenyl	338.38	0	4	3.9	41.90	4	Good	Good
<b>4f</b>	3-fluorophenyl	338.38	0	4	3.9	41.90	4	Good	Good
<b>4g</b>	4-fluorophenyl	338.38	0	4	3.9	41.90	4	Good	Good
<b>4h</b>	5- methylthiophen- 2-yl	340.44	0	4	3.9	70.14	4	Good	Good
<b>4i</b>	furan-2-yl	310.35	0	5	3.0	55.04	4	Good	Good

**Table 2.**  $\alpha$ -Glucosidase inhibition, DPPH and NO radical scavenging activities of the tested diarylpentadienones and their pyrazoline derivatives **3a-j** and **4a-i**. Data presented as mean  $\pm$  SEM



Compound	Ar	$\alpha$ -Glucosidase	DPPH radical scavenging	NO radical scavenging
		IC <sub>50</sub> ( $\mu$ M $\pm$ SEM)	IC <sub>50</sub> ( $\mu$ M $\pm$ SEM) <sup>a</sup>	IC <sub>50</sub> ( $\mu$ M $\pm$ SEM) <sup>a</sup>
<b>3a</b>	Phenyl	ND	56.03 $\pm$ 0.1	25.49 $\pm$ 0.1
<b>3b</b>	3-methoxyphenyl	ND	39.51 $\pm$ 0.1	58.94 $\pm$ 0.2
<b>3c</b>	4-methoxyphenyl	ND	53.81 $\pm$ 0.1	51.74 $\pm$ 0.1
<b>3d</b>	2,4-dimethoxyphenyl	ND	4.06 $\pm$ 0.1	18.89 $\pm$ 0.1
<b>3e</b>	2-fluorophenyl	ND	97.51 $\pm$ 0.2	137.29 $\pm$ 0.9
<b>3f</b>	3-fluorophenyl	ND	74.59 $\pm$ 0.2	1321.10 $\pm$ 0.2
<b>3g</b>	4-fluorophenyl	ND	87.31 $\pm$ 0.2	255.36 $\pm$ 0.8
<b>3h</b>	5-methylthiophen-2-yl	40.52 $\pm$ 2.0	46.52 $\pm$ 0.1	493.16 $\pm$ 0.9
<b>3i</b>	furan-2-yl	ND	53.99 $\pm$ 0.1	1218.49 $\pm$ 0.2
<b>3j</b>	2-fluoro-4-methoxyphenyl	ND	63.42 $\pm$ 0.2	30.60 $\pm$ 0.1
<b>4a</b>	Phenyl	ND	43.32 $\pm$ 0.7	ND
<b>4b</b>	3-methoxyphenyl	ND	74.48 $\pm$ 0.1	ND
<b>4c</b>	4-methoxyphenyl	ND	81.50 $\pm$ 0.3	ND
<b>4d</b>	2,4-dimethoxyphenyl	ND	38.74 $\pm$ 0.1	490.35 $\pm$ 0.5
<b>4e</b>	2-fluorophenyl	ND	42.67 $\pm$ 0.1	211.21 $\pm$ 0.1
<b>4f</b>	3-fluorophenyl	ND	4.58 $\pm$ 0.1	17.61 $\pm$ 0.1
<b>4g</b>	4-fluorophenyl	ND	20.65 $\pm$ 0.5	ND
<b>4h</b>	5-methylthiophen-2-yl	ND	34.16 $\pm$ 0.2	ND
<b>4i</b>	furan-2-yl	ND	58.03 $\pm$ 0.2	ND
	Quercetin <sup>b,c</sup>	-	5.32 $\pm$ 0.0	6.31 $\pm$ 0.0
	Gallic acid <sup>c</sup>	-	-	5.17 $\pm$ 0.0
	Acarbose <sup>d</sup>	543.8 $\pm$ 3.0	-	-

ND = IC<sub>50</sub> is not determined if the percentage of inhibition is less than 50%

<sup>a</sup> The IC<sub>50</sub> is converted from the original unit,  $\mu$ g/mL into  $\mu$ M

<sup>b</sup> Positive standard for both DPPH and NO scavenging assays

<sup>c</sup> Positive standard for the NO scavenging assay

<sup>d</sup> Positive standard for the  $\alpha$ -glucosidase suppression assay, tested at concentration of 500  $\mu$ M

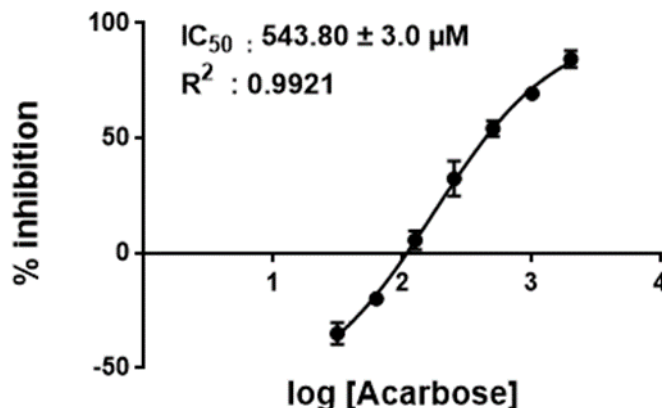


Figure 5. Dose response curve of acarbose on  $\alpha$ -glucosidase inhibition

### Biological Evaluation

All purified and structurally confirmed molecules **3a-j** and **4a-i** were then subjected to several biological assays and discussed in the following sub-sections. All bioactivities resulting from the tested compounds and their respective  $IC_{50}$  values are listed in Table 2.

### $\alpha$ -Glucosidase Inhibition

Nineteen purified diarylpentadienones (**3a-j**) and their pyrazoline derivatives (**4a-i**) were first tested against yeast maltase-isolated  $\alpha$ -glucosidase enzyme at a test concentration of 50  $\mu$ M based on previous procedures under optimal conditions [32, 48]. According to the preliminary evaluation (Table 2), analogue **3h** showed the strongest  $\alpha$ -glucosidase inhibition of 54% with an  $IC_{50}$  value of  $40.52 \pm 2.0$   $\mu$ M in a dose-dependent manner (Figure 4), compared with the standard drug acarbose ( $IC_{50} = 543.80 \pm 3.0$   $\mu$ M, Figure 5). However, the other molecules showed weak inhibition rates in the range of 1-9%, suggesting that these new diarylpentadienones and their pyrazoline derivatives may not possess significant AGI efficacies. The results disclose that the 5-methylthiophenyl moiety plays an important role in the suppression of  $\alpha$ -glucosidase. It is thought to form multiple hydrophobic bonds with the target enzyme via the aromatic  $\pi$ -system, suggesting that the high potential for hydrogen bond formation is insignificant for the inhibition of this specific carbohydrate-hydrolyzing enzyme.

### DPPH and Nitric Oxide Scavenging Activities

The preliminary results of DPPH radical scavenging of compounds **3a-j** and **4a-i** showed that all molecules were able to significantly scavenge DPPH free radicals

with 75% inhibition compared with the nitric oxide (NO) radical (Table 2). Subsequently, the  $IC_{50}$  values of these bioactive compounds were determined and the results were compared with those of quercetin as a positive control. According to the results, compounds **3d** and **4f** exhibited the highest DPPH scavenging activity with  $IC_{50}$  values of  $4.06 \pm 0.1$   $\mu$ M and  $4.58 \pm 0.1$   $\mu$ M, respectively, followed by quercetin ( $IC_{50}$  of  $5.32 \pm 0.0$   $\mu$ M). The presence of the electron donating group (-OCH<sub>3</sub>) at the *ortho* and *para* positions of the phenyl ring of **3d** makes the molecule highly nucleophilic, effectively enhancing its DPPH scavenging properties. Moreover, the *meta*-fluoro moiety on the phenyl ring of pyrazoline analogues **4f** in conjunction with the electron-withdrawing *N*-acetyl group are crucial molecular fragments responsible for the strong antioxidant properties. In contrast, the remaining compounds showed moderate to weak activity with  $IC_{50}$  values ranging from  $20.65 \pm 0.5$  to  $97.51 \pm 0.2$   $\mu$ M.

Continuing our efforts to explore the therapeutic potential of diarylpentadienones and their pyrazoline derivatives, we have prepared additional new compounds (**3b**, **3e**, **3f**, **3j**, **4b-f**, and **4i**) to evaluate their antioxidant capacity, particularly with respect to NO scavenging activity. The NO scavenging efficacy recorded in Table 2 shows that the majority of the tested compounds demonstrated moderate to weak NO scavenging efficacy with  $IC_{50}$  values ranging from  $17.61 \pm 0.1$  to  $1321.10 \pm 0.2$   $\mu$ M compared to the positive controls, quercetin and gallic acid, with  $IC_{50}$  values of  $6.31 \pm 0.0$  and  $5.17 \pm 0.0$   $\mu$ M, respectively. A similar SAR trend was observed for both series of diarylpentadienones and pyrazolines, as compounds **3d** and **4f** also displayed the highest NO scavenging activity with respective  $IC_{50}$  values of  $18.89 \pm 0.1$  and

$17.61 \pm 0.1 \mu\text{M}$ . It is suggested that the di-methoxyl group is a crucial functional group in **3d**, while the meta-fluorinated benzene ring A was observed as a crucial fragment in **4f**.

### Molecular Docking Studies

AutoDock Vina 1.1.2 was used to perform molecular docking simulations to gain detailed insight into the structure and binding mode of the active molecule **3h** as well as **3d** and **4f** in  $\alpha$ -glucosidase and human antioxidant enzymes.

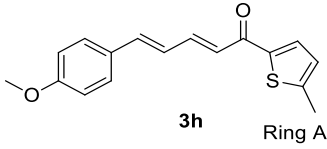
### Molecular Docking of **3h** on Homology Modelled $\alpha$ -Glucosidase Enzyme.

Since the crystal structure of  $\alpha$ -glucosidase from *S. cerevisiae* is currently not publicly available, an  $\alpha$ -glucosidase homology model was constructed using a previously described molecular docking analysis procedure. The isomaltase crystal structure (PDB: 3A4A) from baker's yeast was selected as the prototype for the homology model because of its 72% identity and 84% commonality with the  $\alpha$ -glucosidase from *S. cerevisiae* (Uniprot ID: P53341). The homologous protein was generated based on the MODELER protocol and the Ramachandran plot from RAMPAGE server further validated the optimized structure.

Approximately 98% of the residues were located in the favored regions, while 2% of the residues were located in the allowed regions of the Ramachandran plot. The generated homology model proved to be satisfactory as no outlier residues were detected and an RMSD value of  $0.7147 \text{ \AA}$  was obtained from the re-docking procedure (Figure S4 Supplementary Material) [30]. All involved binding interactions are listed in Table 3.

Based on the rigid docking analysis (Figure 6), the 4-methoxyphenyl was found to form a strong hydrogen bond (green-dashed line) with the Arg439 residue, and stable  $\pi$ -anion and  $\pi$ - $\pi$  T-shaped interactions, with the  $\alpha$ -glucosidase Asp349 and Phe177, respectively. In addition, the 5-methylthiophenyl fragment of analogue **3h** was found to contact residues His279, Glu304, and Arg312 via  $\pi$ -sulphur (orange-dashed line),  $\pi$ -anion (light orange-dashed line), and alkyl (light orange-dashed line) interactions. For comparison, acarbose was also docked at the same binding site in this homology-modelled  $\alpha$ -glucosidase crystal. It was observed that multiple H-bonds are formed between acarbose and Glu276, Glu214, Asn241, as well as Glu304 at the active site. It is probably conceivable that the presence of hydrophobic interactions including  $\pi$ -sulphur and  $\pi$ -alkyl bonds at the active site residues could play a role in the significant  $\alpha$ -glucosidase inhibitory effect of **3h** compared to other analogues and acarbose.

**Table 3.** Data on the interactions resulting from molecular docking of compounds **3h** and acarbose in homology-modelled  $\alpha$ -glucosidase

Structure	Binding Energy (kcal/mol)	Interacting Amino acid residue	Bond type	Bonding distance (Å)
 <p><b>3h</b> Ring A</p>	-6.7	Glu304	$\pi$ -Anion	4.95
		Arg312	Alkyl	3.88
		His279	$\pi$ -Sulfur	4.79
		Phe177	$\pi$ - $\pi$ T-shaped	4.66
		Asp349	$\pi$ -Anion	4.73
		Arg439	H Bond	2.44
		Acarbose	-6.2	Glu276
Glu214	H Bond			2.01
Lys155	Alkyl			4.80
Asn241	H Bond			2.41, 2.59
Glu304	H Bond			2.53

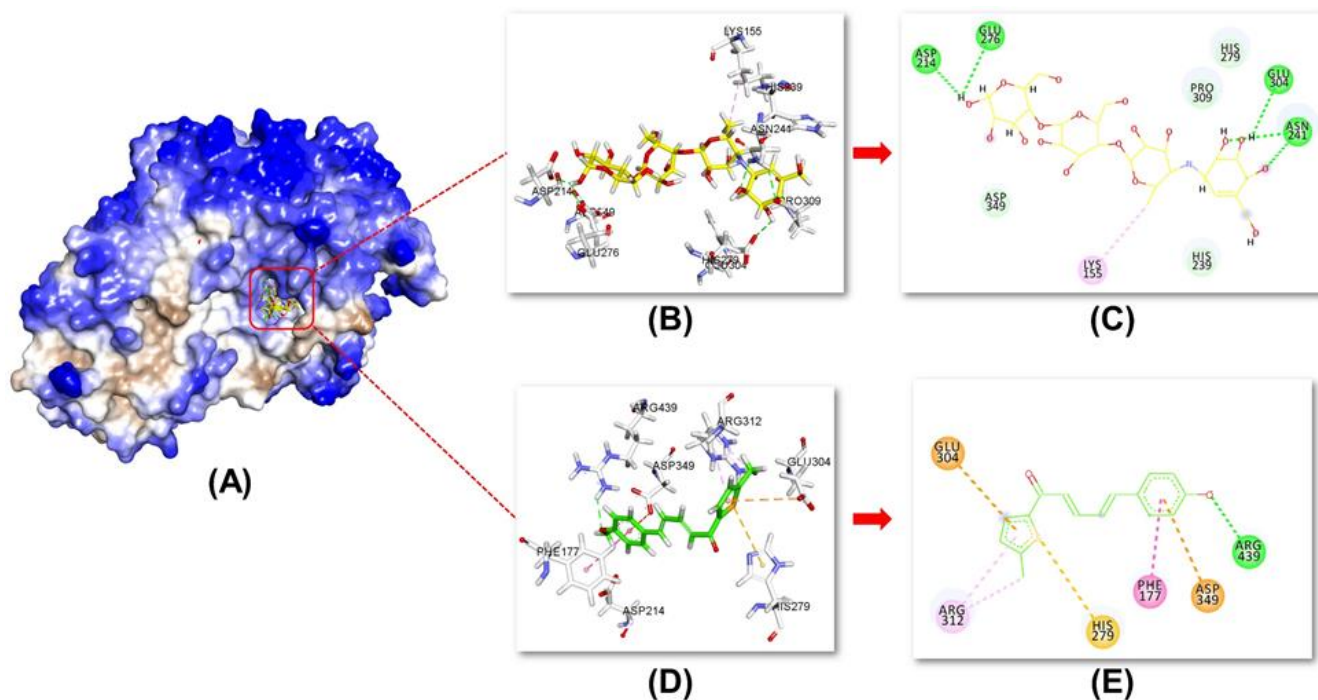


**Figure 6.** Molecular docking model of **3h** and acarbose with the active site of  $\alpha$ -glucosidase. (A) 3D conformational positions of **3h** (yellow) and acarbose (green) in the surface pocket of  $\alpha$ -glucosidase. (B) Key interactions of acarbose at the surface of  $\alpha$ -glucosidase pocket. (C) 2D diagram of acarbose in the surface pocket of  $\alpha$ -glucosidase. (D) Key interactions of **3h** in the surface pocket of  $\alpha$ -glucosidase. (E) 2D diagram of **3h** in the surface pocket of  $\alpha$ -glucosidase. (Green line: H-bond; light green line: carbon H-bond; orange line:  $\pi$ -sulfur; light orange line:  $\pi$ -anion; pink line:  $\pi$ - $\pi$  stacked; light pink line: alkyl)

### Molecular Docking of **3d** and **4f** on Human Antioxidant Enzyme

The synthesized analogues with significant antioxidant properties, **3d** and **4f**, were prepared as rigid ligands for docking simulation to compare their inhibitory affinity toward wild-type human PrxV protein with bound dithiothreitol (DTT) as a competitive inhibitor (PDB ID: 3MNG). The docking validation step was performed, in which DTT was first removed from the 3MNG protein and re-docked to the active site of the PrxV enzyme to obtain the RMSD value of 0.722Å. This step was critical to ensure that the analogues tested bound to the targeted enzymatic sites.

Molecular docking results show strong interactions between active compounds **3d** and **4f** with 3MNG protein, compared with DTT inhibitor (-3.4 kcal/mol). The analogue **4f** shows the strongest binding affinity (-5.7 kcal/mol), which is probably due to the presence of

rotatable bonds of the pyrazoline moiety that increase the flexibility of the ligand to fit into the binding pockets of the 3MNG enzyme, as shown in Figure 7. Moreover, the strong conventional hydrogen bonding (2.60 Å) between the Arg127 residue and the oxygen of *N*-acetyl functionality may also contribute to its significant binding score, confirming the crucial effect of the *N*-acetyl moiety. Moreover, the interaction of **3d** with the enzymatic site of 3MNG indicated the formation of two carbon-hydrogen bonds by the 2,4-dimethoxyl group with Phe43 and Ala42 and resulted in a slightly lower binding affinity of -5.2 kcal/mol than **4f**. On the other hand, the standard quercetin showed a responsive interaction with the target site of the 3MNG protein, but the presence of an unfavourable donor-donor interaction at Thr44 lowered the binding affinity (-5.5 kcal/mol). The 2D and 3D docking representations of DTT, quercetin, **3d** and **4f** analogues are shown in Table 4, while all the binding interactions involved are summarized in Table 5.

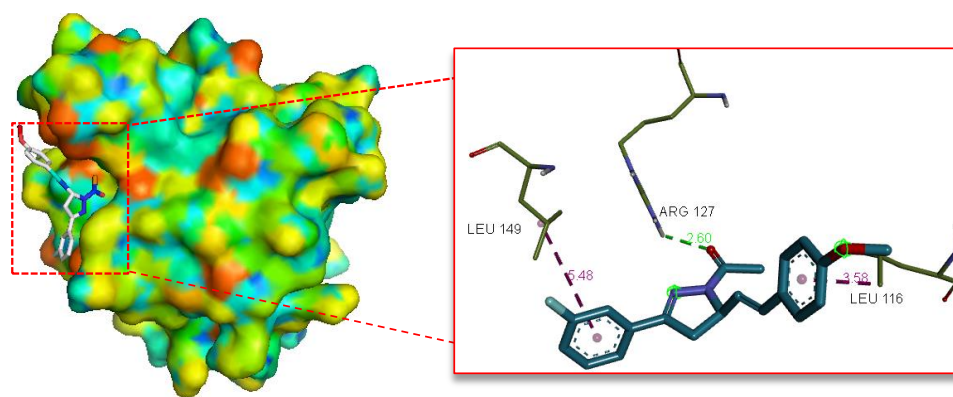
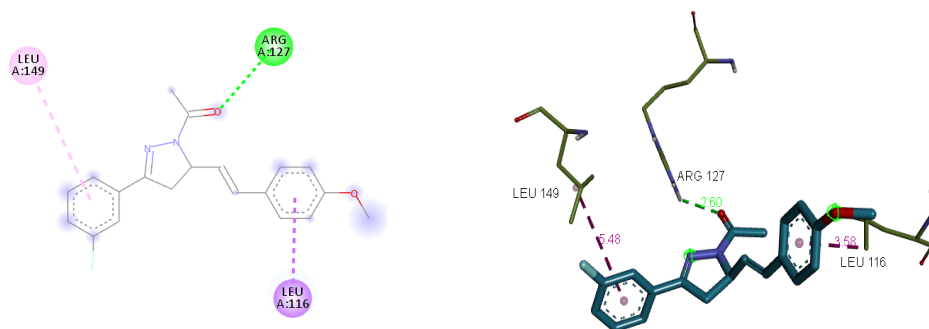


Figure 7. Molecular docking model of **4f** in the 3MNG cavity

Table 4. 2D and 3D diagram of the binding interactions for (A) DTT, (B) quercetin, (C) **3d** and (D) **4f**, as well as respective binding affinity (Green line: H bond; light green line: carbon H-bond; orange line:  $\pi$ -cation; light orange line:  $\pi$ -sulfur; light pink line: alkyl,  $\pi$ -alkyl; purple line:  $\pi$ -sigma; red line: unfavorable donor-donor)

	2-D structure	3-D structure	Binding affinity (kcal/mol)
A			-3.4
B			-5.5
C			-5.2

D



-5.7

**Table 5.** Data of interactions resulting from molecular docking of antioxidant standards DTT and quercetin, as well as compounds **3d** and **4f** with human Prx V 3MNG protein

Structure	Interacting Amino acid residue	Bond type	Bonding distance (Å)
 <b>DTT</b>	Gly46	H Bond	1.99
	Leu116	Alkyl	5.45
	Pro40	Alkyl	5.29
	Phe120	$\pi$ -Sulfur	5.13 5.49
 <b>Quercetin</b>	Arg127	$\pi$ -Cation	4.36
	Pro40	$\pi$ -Alkyl	5.18
	Thr44	Unfavorable donor-donor	1.44
	Leu149	$\pi$ -Alkyl	5.41
	Cys47	H Bond	3.07
 <b>3d</b>	Arg127	$\pi$ -Cation	4.87
	Phe43	H Bond	3.48
	Ala42	H Bond	3.59
 <b>4f</b>	Arg127	H Bond	2.60
	Leu116	$\pi$ -Sigma	3.58
	Leu149	$\pi$ -Alkyl	5.48

## CONCLUSION

In summary, a series of diarylpentadienones (**3a-j**) and their pyrazoline derivatives (**4a-i**), including ten new molecules (**3b**, **3e**, **3f**, **3j**, **4b-f**, and **4i**), were PAINS filtered, chemically prepared and evaluated for their dual anti- $\alpha$ -glucosidase and antioxidant properties. Among the synthesized analogues, compound **3h** showed the strongest anti- $\alpha$ -glucosidase activity, with the 5-methylthiophenyl fragment being crucial in triggering  $\alpha$ -glucosidase activity by molecular docking studies. In addition, compounds **3d** and **4f** showed significant free radical scavenging activity (DPPH and NO) compared with the standards quercetin and gallic acid. Subsequent molecular docking analysis

revealed that **3d**, **4f**, and quercetin form important interactions with amino acid residues of human anti-oxidant enzyme, complementing their biological significance in vitro. It can be concluded that diarylpentadienone (**3a-j**) and its pyrazoline derivatives (**4a-i**) are molecules with potential anti- $\alpha$ -glucosidase and antioxidant properties, but not as dual therapeutic agents, suitable for further chemical modification according to pharmaceutical requirements in the future for the treatment of T2DM.

## ACKNOWLEDGEMENTS

This study was supported by the Putra grant-Putra Young Initiative (IPM) [Reference number GP-IPM/



2016/9480700]. The first author would also like to gratefully acknowledge the support of the Nigerian government for funding his study.

#### REFERENCES

1. Saeedi, P., Petersohn, I., Salpea, P., Malanda, B., Karuranga, S., Unwin, N., Colagiuri, S., Guariguata, L., Motala, A. A., Ogurtsova, K., Shaw, J. E., Bright, D. and Williams, R. (2019) IDF Diabetes Atlas Committee. Global and regional diabetes prevalence estimates for 2019 and projections for 2030 and 2045: Results from the International Diabetes Federation Diabetes Atlas, 9<sup>th</sup> edition. *Diabetes Research and Clinical Practice*, **157**, 107843.
2. Roglic, G. (2016) WHO global report on diabetes: A summary. *International Journal of Noncommunicable Diseases*, **1**, 3–8.
3. Galicia-Garcia, U., Benito-Vicente, A., Jebari, S., Larrea-Sebal, A., Siddiqi, H., Uribe, K. B., Ostolaza, H. and Martín, C. (2019) Pathophysiology of type 2 diabetes mellitus. *International Journal of Molecular Sciences*, **21**, 6275–6308.
4. Sun, H., Li, Y., Zhang, X., Lei, Y., Ding, W., Zhao, X. and Yu P. (2015) Synthesis,  $\alpha$ -glucosidase inhibitory and molecular docking studies of prenylated and geranylated flavones, isoflavones and chalcones. *Bioorganic Medicinal Chemistry Letters*, **25**, 4567–4571.
5. Havale, S. H. and Manojit, P. (2009) Medicinal chemistry approaches to the inhibition of dipeptidyl peptidase-4 for the treatment of type 2 diabetes. *Bioorganic Medicinal Chemistry*, **17**, 1783–1802.
6. Dahlén, A. D., Dashi, G., Maslov, I., Attwood, M. M., Jonsson, J., Trukhan, V. and Schiöth, H. B. (2022) Trends in Antidiabetic Drug Discovery: FDA Approved Drugs, New Drugs in Clinical Trials and Global Sales. *Frontiers in pharmacology*, **12**, 807548.
7. Lee, E. Y., Kaneko, S., Jutabha, P., Zhang, X., Seino, S., Jomori, T., Anzai, N. and Miki, T. (2015) Distinct action of the  $\alpha$ -glucosidase inhibitor miglitol on SCLT3, enteroendocrine cells, and GLPI secretion. *Journal of Endocrinology*, **224**, 205–214.
8. Naquvi, K. J. J., Ahamad, S. R., Mir, M., Ali, and Shuaib, M. (2011) Review on role of natural alpha-glucosidase inhibitors for management of diabetes mellitus. *International Journal of Bio-medical Research*, **2**, 374–380.
9. Bajaj, S., and Khan, A. (2012) Antioxidant and diabetes. *Indian Journal of Endocrinology and Metabolism*, **16**, 267–271.
10. Moharram, H. A., Youssef, M. M. (2014) Methods for determining the antioxidant activity: A review. *Alexandria Journal of Food Science and Technology*, **11**, 31–42.
11. Lobo, V., Patil, A., Phatak, A. and Chandra, N. (2010) Free radicals, antioxidants and functional foods: Impact on human health. *Pharmacognosy Reviews*, **4**, 118–126.
12. Valko, M., Leibfritz, D., Jan, M., Milan, M. and Joshua, T. (2007) Free radicals and antioxidants in normal physiological functions and human disease. *International Journal of Biochemistry and Cellular Biology*, **39**, 44–84.
13. Droge, W. (2002) Free radicals in the physiological control of cell function. *Physiological Reviews*, **82**, 47–95.
14. Lee, J., Koo, N. and Min, D. B. (2004) Reactive oxygen species, aging, and antioxidative nutraceuticals. *Comprehensive Reviews in Food Science and Food Safety*, **3**, 21–33.
15. Pisoschi, A. M. and Negulescu, G. P. (2012) Methods for total antioxidant activity determination: A review. *Biochemistry and Analytical Biochemistry*, **1**, 1–10.
16. Tham, C. L., Liew, C. Y., Lam, K. W., Mohamad, A. S., Kim, M. K., Cheah, Y. K. and Israf, D. A. (2010) A synthetic curcuminoid derivative inhibits nitric oxide and proinflammatory cytokine synthesis. *European Journal of Pharmacology*, **628**, 247–254.
17. Lam, K. W., Tham, C. L., Liew, C. Y., Syahida, A., Rahman, M. B. A., Israf, D. A. and Lajis, N. H. (2012) Synthesis and evaluation of DPPH and anti-inflammatory activities of 2,6-bisbenzylidenecyclohexanone and pyrazoline derivatives. *Medicinal Chemistry Research*, **21**, 333–344.
18. Lee, K. H., Haryani, F., Aziz, A., Syahida, A., Abas, F., Shaari, K. and Lajis, N. H. (2009) Synthesis and biological evaluation of curcumin-like diarylpentanoic acid analogues for anti-inflammatory, antioxidant and anti-tyrosinase activities. *European Journal of Medicinal Chemistry*, **44**, 3195–3200.
19. Abdullah, M. A., Lee, Y. R., Mastuki, S. N., Leong S. W., Wan Ibrahim, W. N., Mohammad

- 30 Faruk Auwal Adam, Mohammad Aidiel Md Razali, Yaya Rukayardi, Siti Nurulhuda Mastuki, Leong Sze Wei, Nadiyah Mad Nasir and Siti Munirah Mohd Faudzi
- Synthesis of Diarylpentadienones and Pyrazoline Derivatives as Potential  $\alpha$ -Glucosidase Inhibitor and Their Antioxidant Activities
- Latif, M. A., Ramli, A. N. M., Mohd Aluwi, M. F. F., Mohd Faudzi, S. M. and Kim C. H. (2020) Development of a new class of diarylpentadienone analogues as anti-diabetic agents: Synthesis, in vitro biological and in vivo toxicity evaluations, and molecular docking analyses. *Bioorganic Chemistry*, **104**, 104277–104291.
20. Sethi, R., Ahuja, M. and Jatolia, S. N. (2015) Pharmacological activities of pyrazoline derivatives. *International Journal of Pharmaceutical Sciences Review and Research*, **34**, 228–233.
21. Naik, N., Kumar, H. V. and Swetha, S. (2011) 1,5-diphenylpenta-1,4 dien-3-ones: a novel class of free radical scavengers. *Bulgarian Chemical Communications*, **43**, 460–464.
22. Christodoulou, M. S., Liekens, S., Kasiotis, K. M. and Haroutounian, S. A. (2010) Novel pyrazole derivatives: synthesis and evaluation of anti-angiogenic activity. *Bioorganic Medicinal Chemistry*, **18**, 4338–4350.
23. Khunt, R. C., Khedkar, V. M., Chawda, R. S., Chauhan, N. A., Parikh, A. R. and Coutinho, E. C. (2012) Synthesis, antitubercular evaluation and 3D QSAR study of N-phenyl-3-(4-fluorophenyl)-4-substituted pyrazole derivatives. *Bioorganic Medicinal Chemistry Letters*, **22**, 666–678.
24. Burguete, A., Pontiki, E., Hadjipavlou-Litina, D. R., Vicente, E., Solano, B., Ancizu, S., Perez-Silanes, S., Aldana, I. and Monge, A. (2007) Synthesis and anti-inflammatory/antioxidant activities of some new ring 3-phenyl-1(1, 4-di-N-oxide quinoxaline-2-yl)-2-propen-1-one derivatives and of their 4, 5-dihydro-(1H)-pyrazole analogues. *Bioorganic Medicinal Chemistry Letters*, **17**, 6439–6443.
25. Babu, V. H., Sridevi, C. H., Joseph, A. and Srinivasan, K. K. (2007) Synthesis and biological evaluation of some new pyrazolines. *Indian Journal of Pharmaceutical Sciences*, **69**, 470–473.
26. Jayaprakash, V., Sinha, B. N., Ucar, G. and Ercan, A. (2008) Pyrazoline-based mycobactin analogues as MAO-inhibitors. *Bioorganic Medicinal Chemistry Letters*, **18**, 6362–6368.
27. Mohd Faudzi, S. M., Leong, S. W., Abas, F., Mohd Aluwi, M. F. F., Rullah, K., Lam, K. W. and Lajis, N. H. (2015) Synthesis, biological evaluation and QSAR studies of diarylpentanoid analogues as potential nitric oxide inhibitors. *Medicinal Chemistry Communication*, **6**, 1069–1080.
28. Lévai, A., Patonay, T., Silva, A. M. S., Pinto, D. C. G. A. and Cavaleiro, J. A. S. (2002) Synthesis of 3-aryl-5-styryl-2-pyrazolines by the reaction of (E,E)-cinnamylideneacetophenones with hydrazines and their oxidation into pyrazoles. *Journal of Heterocyclic Chemistry*, **39**, 751–758.
29. Mohd Faudzi, S. M., Leong, S. W., Auwal, F. A., Abas, F., Wai, L. K., Ahmad, S., Tham, C. L., Shaari, K., Lajis, N. H. and Yamin, B. M. (2020) In-silico studies, nitric oxide and cholinesterase inhibition activities of pyrazoline analogues of diarylpentanoids. *Archiv der Pharmazie*, **354**, e2000161.
30. Lagorce, D., Bouslama, L., Becot, J., Miteva, M. A. and Villoutreix, B. O. (2017) FAF-Drugs4: free ADME-Tox filtering computations for chemical biology and early stages drug discovery. *Bioinformatics*, **33**, 3658–3660.
31. Laskowski, R. A., Rullmann, J. A. C., MacArthur, M. W., Kaptein, R. and Thamton, J. M. (1996) AQUA and PROCHECK-NMR: programs for checking the quality of protein structures solved by NMR. *Journal of Biomolecular NMR*, **8**, 477–486.
32. Samardi, B., Aminuddin, F., Hamid, M., Saari, N., Abdulhamid, A. and Ismail, A. (2012) Hypoglycemic effect of cocoa (*Theobroma cacao* L) autolysates. *Food Chemistry*, **134**, 905–911.
33. Auld, D. S., Inglese, J. and Dahlin, J. L. (2004) Assay interference by aggregation, in: Markossian, S., Sittampalam, G. S., Grossman, A., Brimacombe, K., Arkin, M., Auld, D., Austin, C. P., Baell, J., Caaveiro, J. M. M., Chung, T. D. Y., Coussens, N. P., Dahlin, J. L., Devanaryan, V., Foley, T. L., Glicksman, M., Hall, M. D., Haas, J. V., Hoare, S. R. J., Inglese, J., Iversen, P. W., Kahl, S. D., Kales, S. C., Kirshner, S., Lal-Nag, M., Li, Z., McGee, J., McManus, O., Riss, T., Saradjian, P., Trask, O. J. Jr., Weidner, J. R., Wildey, M. J., Xia, M., Xu, X. (Eds.), Assay Guidance Manual [Internet]. Bethesda (MD): Eli Lilly & Company and the National Center for Advancing Translational Science.
34. Abdullah, M. A., Lee, Y., Mastuki, S. N., Leong, S. W., Ibrahim, W. N. W., Latif, M. A. M., Ramli, A. N. M. R., Mohd Aluwi, M. F. F., Mohd Faudzi, S. M. and Kim, C. H. (2020) Development of diarylpentadienone analogues as alpha-glucosidase inhibitor: synthesis, in vitro and in vivo toxicity evaluations and molecular docking analysis. *Bioorganic Chemistry*, **104**, 102277.
35. Wan, C., Yuan, T., Cirello, A. L. and Seeram, N. P. (2012) Antioxidant and  $\alpha$ -glucosidase inhibitory phenolics isolated from highbush blueberry flowers. *Food Chemistry*, **135**, 1929–1937.
36. Abd Ghafar, S. Z., Mediani, A., Maulidiani, Ramli, N. S. and Abas, F. (2018) Antioxidant,  $\alpha$ -glucosidase, and nitric oxide inhibitory activities

- of *Phyllanthus acidus* and LC–MS/MS profile of the active extract. *Food Bioscience*, **25**, 134–140.
37. Leong, S. Z., Abas, F., Lam, K. W. and Yusoff, K. (2018) In vitro and in silico evaluation of diarylpentanoic acid series as  $\alpha$ -glucosidase inhibitor. *Bioorganic Medicinal Chemistry Letters*, **28**, 302–309.
38. Trott, O. and Olson, A. J. (2010) Autodock: improving the speed and accuracy of docking with a new scoring function, efficient optimization and multithreading. *Journal of Computational Chemistry*, **31**, 455–461.
39. Baell, J. B. (2015) Screening-based translation of public research encounters painful problems. *ACS Medicinal Chemistry Letters*, **6**, 229–234.
40. Baell, J. B. (2013) Broad coverage of commercially available lead-like screening space with fewer than 350,000 compounds. *Journal of Chemical Information and Modeling*, **53**, 39–55.
41. Baell, J. B. and Holloway, G. A. (2010) New substructure filters for removal of pan assay interference compounds (PAINS) from screening libraries and for their exclusion in bioassays. *Journal of Medicinal Chemistry*, **53**, 2719–2740.
42. Jasial, S., Hu, Y. and Bajorath, J. (2017) How frequently are Pan-assay interference compounds active? large-scale analysis of screening data reveals diverse activity profiles, low global hit frequency, and many consistently inactive compounds. *Journal of Medicinal Chemistry*, **60**, 3879–3886.
43. Baell, J. B. and Nissink, J. W. M. (2018) Seven-year itch: Pan-assay interference compounds (PAINS) in 2017 - Utility and limitations. *ACS Chemical Biology*, **13**, 36–44.
44. Viviani, L. G., Piccirillo, E., Cheffer, A., de Rezende, L., Ulrich, H., Carmona-Ribeiro, A. M. and Amaral, A. T. (2018) Be aware of aggregators in the search for potential human ecto-5-nucleotidase inhibitors. *Molecules*, **23**, 1876–1890.
45. McGovern, S. L., Helfand, B. T., Feng, B. K. and Shoichet, B. K. (2003) A specific mechanism of nonspecific inhibition. *Journal of Medicinal Chemistry*, **46**, 4265–4272.
46. Veber, D. F., Johnson, S. R., Cheng, H. Y., Smith, B. R., Ward, K. W. and Kopple, K. D. (2002) Molecular properties that influence the oral bioavailability of drug candidates. *Journal of Medicinal Chemistry*, **45**, 2615–2623.
47. Markham, A. (2017) Baricitinib: first global approval. *Drugs*, **77**, 697–704.
48. Kim, J. S., Kwon, C. S. and Son, K. H. (2000) Hypoglycemic effect of cocoa (*Theobroma cacao* L.) autolysates. *Bioscience, Biotechnology and Biochemistry*, **64**, 2458–2461.